Continuation and collapse of homoclinic tangles

Wolf-Jürgen Beyn* Thorsten Hüls*
Department of Mathematics, Bielefeld University
POB 100131, 33501 Bielefeld, Germany
beyn@math.uni-bielefeld.de huels@math.uni-bielefeld.de

June 3, 2012

Abstract

By a classical theorem transversal homoclinic points of maps lead to shift dynamics on a maximal invariant set, also referred to as a homoclinic tangle. In this paper we study the fate of homoclinic tangles in parameterized systems from the viewpoint of numerical continuation and bifurcation theory. The new bifurcation result shows that the maximal invariant set near a homoclinic tangency, where two homoclinic tangles collide, can be characterized by a system of bifurcation equations that is indexed by a symbolic sequence. These bifurcation equations consist of a finite or infinite set of hilltop normal forms known from singularity theory. For the Hénon family we determine numerically the connected components of branches with multi-humped homoclinic orbits that pass through several tangencies. The homoclinic network found by numerical continuation is explained by combining our bifurcation result with graph-theoretical arguments.

Keywords: Homoclinic tangency, symbolic dynamics, numerical continuation, bifurcation of homoclinic orbits.
AMS Subject Classification: 37N30, 65P20, 65P30

1 Introduction

We consider parameter dependent, discrete time dynamical systems of the form

$$x_{n+1} = f(x_n, \lambda), \quad n \in \mathbb{Z}, \tag{1.1}$$

*Supported by CRC 701 'Spectral Structures and Topological Methods in Mathematics'.

where f is smooth and $f(\cdot,\lambda), \lambda \in \mathbb{R}$ are diffeomorphisms in $\mathbb{R}^k$. We assume that the system (1.1) has a smooth branch of hyperbolic fixed points and our main interest is in branches of homoclinic orbits that return to these fixed points. Generically one finds turning points on these branches which correspond to homoclinic tangencies where stable and unstable manifolds of the fixed point intersect nontransversally, see [26, 3] for the precise relation.

While the dynamics near transversal intersections are well understood through the celebrated Smale-Shilnikov-Birkhoff Theorem (see [43, 42, 18, 36]), the picture near homoclinic tangencies still seems to be far from being complete. There is a wealth of references that deal with phenomena occurring near homoclinic tangencies, mostly for planar diffeomorphisms. We mention the two monographs [35, 5] which deal with various aspects of nonuniformly hyperbolic behavior, such as the Newhouse phenomenon, measures of sets with secondary tangencies etc. Another source showing the richness of phenomena is [6] where the authors study the so-called fattened Arnold map as a model for tangencies of planar diffeomorphisms. We also refer to the work [15] which supports the generic occurrence of homoclinic tangencies of all orders. Among the further references, we mention the papers [7, 9, 8] which relate homoclinic tangencies to global structural changes, such as boundary crisis or basin boundary metamorphosis. Moreover, a theory of trellises (sets of pieces of stable and unstable manifolds) is developed that allows to study global changes in two-dimensional phase space by symbolic coding and graph representations. In [28] it is shown that shift dynamics occurs in arbitrarily small neighborhoods of the tangency.

Homoclinic (or heteroclinic) tangencies also occur in a natural way for Poincaré maps of continuous time dynamical systems. These maps are either generated by classical Poincaré sections of periodic orbits or by special cross-sections taken in the vicinity of continuous homoclinic orbits. We refer to [22, Ch.4,5] for a recent overview and to [31, 29, 34] for numerical approaches utilizing such sections. In particular, these references study codimension-two homoclinic orbits ('orbit flip' and 'inclination flip') which lead to multi-humped orbits in a fan of the two-parameter region. More details on the relation to continuous systems will be discussed in Section 2.

Finally, we mention that transversal and tangential homoclinic orbits of maps can be computed numerically in a robust way by solving boundary value problems on a finite interval, cf. [4, 13, 16, 26]. Errors caused by this approximation have been completely analyzed, see [27, 26, 3]. The works [26, 16] also study curves of homoclinic tangencies in two-parameter systems.

To the best of our knowledge the maximal invariant set near a homoclinic tangency has not been completely characterized in the literature. Nor are we aware of any study – particularly for Hénon's map – of global connected components of multi-humped homoclinic orbits containing tangencies. Both topics will be central to this paper. We consider bifurcations of multi-humped homoclinic orbits from tangential orbits in arbitrary space dimensions and investigate

in detail the global behavior of branches of multi-humped orbits for the classical Hénon example.

Our main local result (see Theorem 1) determines the elements of the maximal invariant set in a neighborhood of the tangent orbit and of the critical parameter from a set of bifurcation equations. Using the same shift space as in the transversal case, we associate with any sequence of symbols a bifurcation equation that describes those branches of orbits that have the return pattern of the symbolic sequence. Such a result does not fully resolve the dynamics near tangencies, but reduces the problem to a set of perturbed bifurcation equations for which the unperturbed form is known (similar to Liapunov-Schmidt reduction, cf. [14, Ch.I]). The theorem covers multi-humped homoclinic orbits that enter and leave a neighborhood of the fixed point several times, by relating it to a perturbed system of hilltop bifurcations (see [14] for the hilltop normal form). Our main results will be stated in Section 2 (Theorems 1 and 5) with the rather involved proofs deferred to Sections 5 and 6.

The global approach asks for possible bifurcations of multi-humped orbits that are known to emerge from the tangencies. We take the Hénon family as a model equation for a detailed numerical study of the homoclinic network that arises from a total of 4 primary homoclinic tangencies. We show that the connected components of this network are by no means arbitrary. Rather, they follow certain rules governing the bifurcations of multi-humped orbits. Combining these rules with graph-theoretical and combinatorial arguments allows to predict the structure to a large extent, see Theorem 9. Only some fine details are left to numerical computations as will be demonstrated in Sections 3 and 4.

2 Setting of the problem and main results

The aim of this section is to state our main result on bifurcation equations near homoclinic tangencies. We first describe the setting and state our assumptions:

A1 $f \in \mathcal{C}^\infty(\mathbb{R}^k \times \Lambda_0, \mathbb{R}^k)$ for some open set $\Lambda_0 \subset \mathbb{R}$ and $f(\cdot, \lambda)$ is a diffeomorphism for all $\lambda \in \Lambda_0$,

A2 $f(\xi(\lambda), \lambda) = \xi(\lambda)$ for some smooth branch $\xi(\lambda) \in \mathbb{R}^k, \lambda \in \Lambda_0$,

A3 $f_x(\xi(\lambda), \lambda) \in \mathbb{R}^{k,k}$ is hyperbolic for all $\lambda \in \Lambda_0$.

Clearly, if ξ_0 is a hyperbolic fixed point of $f(\cdot, \lambda_0)$ for some $\lambda_0 \in \mathbb{R}$ then **A2** and **A3** follow for some neighborhood Λ_0 of λ_0. Replacing f by $g(x, \lambda) = f(x + \xi(\lambda + \lambda_0), \lambda + \lambda_0) - \xi(\lambda + \lambda_0)$ shows that **A2**, **A3** can be assumed to hold for the trivial branch $\xi(\lambda) = 0$ and for a neighborhood Λ_0 of zero. This will be our standing assumption throughout Sections 5 and 6.

It is well known that transversal homoclinic orbits lead to chaotic dynamics on a nearby invariant set commonly referred to as a homoclinic tangle. Let us first assume that this situation occurs at some parameter value $\tilde{\lambda} \in \Lambda_0$.

A4 For some $\tilde{\lambda} \in \Lambda_0$ there exists a nontrivial homoclinic orbit $\tilde{x}_{\mathbb{Z}} = (\tilde{x}_n)_{n\in\mathbb{Z}}$, i.e. $\lim_{n\to\pm\infty} \tilde{x}_n = \tilde{\xi} := \xi(\tilde{\lambda})$ and $\tilde{x}_n \neq \tilde{\xi}$ for some $n \in \mathbb{Z}$. This orbit is *transversal* in the sense that the variational equation

$$y_{n+1} = f_x(\tilde{x}_n, \tilde{\lambda})y_n, \quad n \in \mathbb{Z} \tag{2.1}$$

has no nontrivial bounded solution $y_{\mathbb{Z}} = (y_n)_{n\in\mathbb{Z}}$ in $\mathbb{R}^k$.

In this case the stable and the unstable manifold of $\tilde{\xi}$ intersect transversally at each $\tilde{x}_n$ and the set $\tilde{H} = \{\tilde{x}_n\}_{n\in\mathbb{Z}} \cup \{\tilde{\xi}\}$ is hyperbolic, cf. [37]. Moreover, there exists an open neighborhood U of $\tilde{H}$ such that the dynamics on the maximal invariant set

$$M(U, \tilde{\lambda}) = \{x \in U : f^n(x, \tilde{\lambda}) \in U \ \forall n \in \mathbb{Z}\} \tag{2.2}$$

is conjugate to a subshift of finite type (see the Smale-Shilnikov-Birkhoff Homoclinic Theorem in [18] and [36, Chapter 5] for a proof). To be precise, let $N \geq 2$ and let

$$S_N = \{0, 1, \ldots, N-1\}^{\mathbb{Z}}$$

be the shift space with N symbols which is compact w.r.t. the metric

$$d(s,t) = \sum_{j\in\mathbb{Z}} 2^{-|j|}|s_j - t_j|, \quad s = (s_j)_{j\in\mathbb{Z}}, t = (t_j)_{j\in\mathbb{Z}} \in S_N. \tag{2.3}$$

Let β be the Bernoulli shift

$$\beta(s)_i = s_{i+1}, \quad i \in \mathbb{Z}, \quad s \in S_N.$$

Consider a special subshift of finite type, see [32]

$$\Omega_N = \{s \in S_N : A^{(N)}_{s_i, s_{i+1}} = 1 \ \forall i \in \mathbb{Z}\}$$

generated by the $N \times N$ binary matrix

$$A^{(N)} = \begin{pmatrix} 1 & 1 & 0 & \cdots & 0 \\ 0 & 0 & 1 & \ddots & \vdots \\ \vdots & & \ddots & 1 & 0 \\ 0 & & & \ddots & 1 \\ 1 & 0 & \cdots & \cdots & 0 \end{pmatrix} \in \{0,1\}^{N\times N}.$$

Then there exists a neighborhood U of $\tilde{H}$, an integer $N \geq 2$ and a homeomorphism $h : \Omega_N \to M(U, \tilde{\lambda})$ such that

$$f(\cdot, \tilde{\lambda}) \circ h = h \circ \beta \quad \text{in } \Omega_N. \tag{2.4}$$

A continuation of the transversal homoclinic orbit w.r.t. the parameter λ leads to a curve of homoclinic orbits that typically exhibits turning points. As an example we refer to Figure 1 for the Hénon map. Parts of the branch that can be parametrized by λ belong to transversal homoclinic orbits while (quadratic) turning points correspond to homoclinic orbits with a (quadratic) tangency, see Theorem 3 for a precise statement. In this case we replace Assumption **A4** by

B4 For some $\bar{\lambda} \in \Lambda_0$ there exists a nontrivial homoclinic orbit $\bar{x}_{\mathbb{Z}} = (\bar{x}_n)_{n\in\mathbb{Z}}$ converging towards $\bar{\xi} = \xi(\bar{\lambda})$. The orbit is *tangential* in the sense that the variational equation

$$y_{n+1} = f_x(\bar{x}_n, \bar{\lambda})y_n, \quad n \in \mathbb{Z} \tag{2.5}$$

has a non-trivial bounded solution $u_{\mathbb{Z}} = (u_n)_{n\in\mathbb{Z}}$ in $\mathbb{R}^k$ that is unique up to constant multiples.

Since the fixed point stays hyperbolic we have exponential decay for both the orbit and the solution of (2.5), i.e. for some $\alpha, C_e > 0$

$$\|\bar{x}_n - \bar{\xi}\| + \|u_n\| \le C_e \mathrm{e}^{-\alpha|n|}, \quad n \in \mathbb{Z}. \tag{2.6}$$

Therefore, we may normalize

$$\|u_{\mathbb{Z}}\|_{\ell^2}^2 = \langle u_{\mathbb{Z}}, u_{\mathbb{Z}}\rangle_{\ell^2}^2 = \sum_{n\in\mathbb{Z}} u_n^T u_n = 1. \tag{2.7}$$

In the following we use $\langle\cdot,\cdot\rangle$ to denote the inner product in ℓ^2. The assumption on (2.5) in **B4** holds if and only if the tangent spaces of the stable and unstable manifold have a one-dimensional intersection, i.e.

$$T_{\bar{x}_n} W^s(\bar{\xi}) \cap T_{\bar{x}_n} W^u(\bar{\xi}) = \mathrm{span}(\bar{u}_n), \quad n \in \mathbb{Z}.$$

We refer to Theorem 3 and to [26, Appendix] for a more general statement.

Consider open neighborhoods $U \subset \mathbb{R}^k$ of $H = \{\bar{x}_n\}_{n\in\mathbb{Z}} \cup \{\bar{\xi}\}$ and $\Lambda \subset \Lambda_0$ of $\bar{\lambda}$, respectively. Our main interest is in the dynamics on the maximal invariant set

$$M(U, \Lambda) = \{(x, \lambda) \in U \times \Lambda : f^n(x, \lambda) \in U \ \forall n \in \mathbb{Z}\}.$$

As in the transversal case, we will still work with the subshift (Ω_N, β) but the conjugacy (2.4) will be replaced by a set of bifurcation equations. For any $s \in \Omega_N$ define the index set

$$I(s) = \{n \in \mathbb{Z} : s_n = 1\}, \tag{2.8}$$

and note that $I : \Omega_N \to \mathbb{Z}(N) \subset 2^{\mathbb{Z}}$ is bijective, where

$$\mathbb{Z}(N) = \{J \subset \mathbb{Z} : |j - k| \ge N \ \forall j, k \in J, j \ne k\}. \tag{2.9}$$

With any $s \in \Omega_N$ we associate the Banach space

$$\ell^\infty(s) = \{\tau \in \mathbb{R}^{I(s)} : \|\tau\|_\infty < \infty\},$$

$$\|\tau\|_\infty = \sup_{\ell \in I(s)} |\tau_\ell|, \quad B_\rho = \{\tau \in \ell^\infty(s) : \|\tau\|_\infty \le \rho\}.$$

Our aim is to determine the elements of $M(U, \Lambda)$ from a set of bifurcation equations

$$g_s(\tau, \lambda) = 0, \quad \tau \in B_{\rho_\tau}, \lambda \in \Lambda, \tag{2.10}$$

where $s \in \Omega_N$, $\rho_\tau > 0$ is independent of s and

$$g_s : \begin{array}{ccc} B_{\rho_\tau} \times \Lambda & \to & \ell^\infty(s) \\ (\tau, \lambda) & \mapsto & g_s(\tau, \lambda) \end{array}$$

is a sufficiently smooth map. Note that (2.10) constitutes a finite or an infinite system of equations depending on the cardinality of $I(s)$.

In order to formulate the precise statement we define the pseudo orbits

$$p_n(s) = \bar{\xi} + \sum_{\ell \in I(s)} (\bar{x}_{n-\ell} - \bar{\xi}), \quad n \in \mathbb{Z}. \tag{2.11}$$

Equation (2.6) shows that $p_{\mathbb{Z}}(s)$ is a bounded sequence, in particular

$$\|p_n(s) - \bar{\xi}\| \le \bar{C} = C_e \frac{1 + \mathrm{e}^{-\alpha}}{1 - \mathrm{e}^{-\alpha}}, \quad n \in \mathbb{Z}. \tag{2.12}$$

Setting $\bar{\xi}_n = \bar{\xi}$ for all $n \in \mathbb{Z}$ we write (2.11) more formally as

$$p_{\mathbb{Z}}(s) = \bar{\xi}_{\mathbb{Z}} + \sum_{\ell \in I(s)} \beta^{-\ell} (\bar{x}_{\mathbb{Z}} - \bar{\xi}_{\mathbb{Z}}).$$

Here and in what follows we use the symbol β to denote the shift of sequences in $\mathbb{R}^k$. Thus β acts as an operator in sequence spaces such as $\ell^p(\mathbb{R}^k), 1 \le p \le \infty$.

Similarly, for every $\tau \in \ell^\infty(s)$ we define the bounded sequence

$$v_{\mathbb{Z}}(s, \tau) = \sum_{\ell \in I(s)} \tau_\ell \beta^{-\ell} u_{\mathbb{Z}}. \tag{2.13}$$

Note that the sequence $p_{\mathbb{Z}}(s)$ has humps at the positions defined by $I(s)$ and that $p_{\mathbb{Z}}(s)$ is a pseudo orbit of $f(\cdot, \bar{\lambda})$ with a small error, see Lemma 13. The term $v_{\mathbb{Z}}(s, \tau)$ shifts the solution of the variational equation to the positions defined by $I(s)$ and combines them linearly.

Theorem 1 *Let assumptions* **A1 - A3** *and* **B4** *hold. Then there exist constants* $0 < r_\tau \le \rho_\tau$, $N \in \mathbb{N}$ *and neighborhoods* U *of* H, Λ *of* $\bar\lambda$ *and for any* $s \in \Omega_N$ *smooth functions*

$$\begin{aligned} g_s &: B_{\rho_\tau} \times \Lambda \to \ell^\infty(s), \\ x_{\mathbb{Z},s} &: B_{\rho_\tau} \times \Lambda \to \ell^\infty(\mathbb{R}^k) \end{aligned}$$

with the following properties.

(i) For any point $(y_0, \lambda) \in M(U, \Lambda)$ *with orbit* $y_n = f^n(y_0, \lambda)$, $n \in \mathbb{Z}$ *there exists an index* $\nu \in \mathbb{Z}$ *and elements* $s \in \Omega_N$, $\tau \in B_{\rho_\tau} \subset \ell^\infty(s)$ *such that*

$$\beta^\nu y_{\mathbb{Z}} = x_{\mathbb{Z},s}(\tau, \lambda) + p_{\mathbb{Z}}(s) + v_{\mathbb{Z}}(s, \tau), \tag{2.14}$$

$$g_s(\tau, \lambda) = 0. \tag{2.15}$$

(ii) Conversely, if $s \in \Omega_N$, $\tau \in B_{r_\tau} \subset \ell^\infty(s)$, $\lambda \in \Lambda$ *satisfy* (2.15), *then there exists* $\nu \in \mathbb{Z}$ *such that* $(y_n, \lambda)_{n\in\mathbb{Z}}$, *with* $y_{\mathbb{Z}}$ *given by* (2.14), *belongs to* $M(U, \Lambda)$.

Remark 2 *Theorem 1 reduces the study of* $M(U, \Lambda)$ *to the set of bifurcation equations* (2.15) *with a symbolic index* $s \in \Omega_N$. *It may be regarded as a type of Liapunov-Schmidt reduction though we have not formally put it into this framework. The construction of the neighborhood* $U \times \Lambda$ *uses some features from the transversal case [36, Theorem 5.1], but is considerably more involved, see Sections 5 and 6. We also note that we were not able to prove that one can take* $r_\tau = \rho_\tau$ *which would give a complete characterization of* $M(U, \Lambda)$ *in terms of* (2.14), (2.15). *Another issue which has not yet been resolved, is continuous dependence of the functions* $x_{\mathbb{Z},s}$ *and* g_s *on the symbolic sequence* s *with respect to the metric* (2.3).

The functions g_s and $x_{\mathbb{Z},s}$ have several properties that we discuss next.
Due to **B4** the adjoint equation

$$y_{n+1}^T f_x(\bar x_{n+1}, \bar\lambda) = y_n^T, \quad n \in \mathbb{Z} \tag{2.16}$$

has a non-trivial solution $w_{\mathbb{Z}}$ that is unique up to constant multiples, cf. [37, Section 2]. It decays exponentially as in (2.6) and can thus be normalized such that $\|w_{\mathbb{Z}}\|_{\ell^2} = 1$. Without loss of generality we take C_e in (2.6) such that

$$\|w_n\| \le C_e \mathrm{e}^{-\alpha|n|}, \quad n \in \mathbb{Z}. \tag{2.17}$$

As is shown in [26] the quantities

$$c_\lambda = \langle w_{\mathbb{Z}}, (f_\lambda(\bar x_n, \bar\lambda))_{n\in\mathbb{Z}}\rangle, \quad c_x = \frac{1}{2}\langle w_{\mathbb{Z}}, (f_{xx}(\bar x_n, \bar\lambda)u_n^2)_{n\in\mathbb{Z}}\rangle \tag{2.18}$$

characterize the behavior of the branch of homoclinic orbits that passes through $(\bar x_{\mathbb{Z}}, \bar\lambda)$.

Theorem 3 *The operator $F : \ell^\infty(\mathbb{R}^k) \times \mathbb{R} \to \ell^\infty(\mathbb{R}^k)$ defined by*

$$F(x_{\mathbb{Z}}, \lambda) = \big((x_{n+1} - f(x_n, \lambda))_{n\in\mathbb{Z}}\big) \tag{2.19}$$

has a limit point at $(\bar{x}_{\mathbb{Z}}, \bar{\lambda})$ in the sense that $F(\bar{x}_{\mathbb{Z}}, \bar{\lambda}) = 0$ and

$$\mathcal{N}(D_x F(\bar{x}_{\mathbb{Z}}, \bar{\lambda})) = \operatorname{span}\{u_{\mathbb{Z}}\}.$$

The limit point is transversal, i.e.

$$D_\lambda F(\bar{x}_{\mathbb{Z}}, \bar{\lambda}) \notin \mathcal{R}(D_x F(\bar{x}_{\mathbb{Z}}, \bar{\lambda})) \quad \text{if and only if} \quad c_\lambda \neq 0.$$

Moreover, it is a quadratic turning point, i.e.

$$D_x^2 F(\bar{x}_{\mathbb{Z}}, \bar{\lambda}) u_{\mathbb{Z}}^2 \notin \mathcal{R}(D_x F(\bar{x}_{\mathbb{Z}}, \bar{\lambda})) \quad \text{if and only if} \quad c_x \neq 0.$$

Remark 4 *For transversal homoclinic orbits ($\lambda \neq \bar{\lambda}$), the Sacker-Sell spectrum, cf. [39], of the variational equation* (2.1) *is a pure point spectrum*

$$\Sigma_{\mathrm{ED}}(\lambda) = \{|\mu| : \mu \in \sigma(f_x(\xi(\lambda), \lambda))\}.$$

At a turning point, we find a spectral explosion to a continuous Sacker-Sell spectrum

$$\Sigma_{\mathrm{ED}}(\bar{\lambda}) = \{|\mu| : \mu \in \sigma(f_x(\bar{\xi}, \bar{\lambda}))\} \cup [\mu_s, \mu_u],$$

where

$$\mu_s = \max\{|\mu| < 1 : \mu \in \sigma(f_x(\bar{\xi}, \bar{\lambda}))\}, \quad \mu_u = \min\{|\mu| > 1 : \mu \in \sigma(f_x(\bar{\xi}, \bar{\lambda}))\}.$$

Our second result shows that the constants c_λ, c_x play an important role in the behavior of the bifurcation function $g_s(\tau, \lambda)$.

Theorem 5 *Let the assumptions of Theorem 1 hold. Then the functions $x_{\mathbb{Z},s}$, g_s have the following properties*

(i)

$$x_{\mathbb{Z},\beta s}(\beta\tau, \lambda) = \beta x_{\mathbb{Z},s}(\tau, \lambda), \quad \text{where } I(\beta s) = I(s) - 1, \tag{2.20}$$

$$g_{\beta s}(\beta\tau, \lambda) = \beta g_s(\tau, \lambda). \tag{2.21}$$

(ii) For some constants $C > 0$, $\alpha > 0$, independent of s, N and $\ell \in I(s)$

$$\big|g_s(\tau, \lambda)_\ell - (c_\lambda(\lambda - \bar{\lambda}) + c_x \tau_\ell^2)\big| \leq C\big((\lambda - \bar{\lambda})^2 + |\lambda - \bar{\lambda}| \|\tau\|_\infty + \|\tau\|_\infty^3 + \mathrm{e}^{-\alpha N/2}\big). \tag{2.22}$$

Remark 6 *Note that one can prove existence of n-humped orbits in the transversal case from the well-known shadowing principle, see the remarks following Eq.* (4.1)*. To obtain an analogous result for the tangential case is much more difficult. Although Theorem 1 completely characterizes the maximal invariant set near a tangency, such a result requires to prove existence of smooth solution branches for the reduced system* (2.15)*. In principle, this task is solved by the unfolding theory for singularities, see [14]. However, in order to make the theory applicable to the bifurcation equations* (2.15) *one needs estimates of (all) derivatives of* g_s *in* (2.22)*. In fact, the function* $g_s(\cdot,\cdot)$ *comes out smoothly from Theorem 11, but estimating their derivatives is quite involved (cf. the proof of* (2.22) *in Section 6) and has not yet been done.*

If we consider a homoclinic symbol $s \in \Omega_N$ with $K = \mathrm{card}(I(s)) < \infty$ humps, then Theorem 5 shows that the bifurcation equations are small perturbations of a set of K identical turning point equations

$$0 = c_\lambda(\lambda - \bar{\lambda}) + c_x\tau_\ell^2, \quad \ell \in I(s).$$

If $c_\lambda, c_x \neq 0$ one can shift $\bar{\lambda}$ to zero and scale λ and τ_ℓ such that one obtains a set of hilltop bifurcations of order K, cf. [14, Ch. IX, §3],

$$0 = \lambda - \tau_\ell^2, \quad \ell \in I(s). \tag{2.23}$$

For two-humped orbits the set $I(s)$ contains two elements and the solution curves of (2.23) are shown in Figure 8. This case will be crucial for understanding the global behavior of homoclinic curves in the next sections.

Remark 7 *The emergence of multi-humped homoclinic orbits near tangencies is reminiscent of the fan of multi-humped orbits created near codimension-two homoclinics in continuous systems, see [22, Sect. 5.1] and [40, 21]. However, the underlying mechanisms seem to be different. This is discussed in the survey paper [22, Sect. 4.3] which also suggests to further compare both phenomena. For continuous systems the occurrence of a fan of homoclinics near an inclination flip or orbit flip bifurcation is explained by a so-called singular horse-shoe appearing in suitable Poincaré sections. On the other hand multi-humped orbits in discrete systems are created by maps of horse-shoe type with tangencies. Though it is natural that the codimensions of both phenomena differ by one, there is another distinguishing feature that is relevant for numerical continuation: the curves of multi-humped homoclinics in the fan of a continuous system all accumulate at a single pair of parameters, while the corresponding curves in the discrete system have their own turning points which relate to secondary tangencies close to but not at the critical parameter value. This will be illustrated in Section 4.*

3 Homoclinic orbits and their continuation

A typical example, which plays the role of a normal form for quadratic two-dimensional mappings, is the famous Hénon map, cf. [20, 33, 11, 19] which is defined as

$$f(x,\lambda) = \begin{pmatrix} 1 + x_2 - 1.4x_1^2 \\ \lambda x_1 \end{pmatrix}.$$

This map has fixed points

$$\xi_\pm(\lambda) = \begin{pmatrix} \nu(\lambda) \\ \lambda\nu(\lambda) \end{pmatrix}, \quad \text{where } \nu(\lambda) = \frac{1}{2.8}\left(\lambda - 1 \pm \sqrt{(\lambda-1)^2 + 5.6}\right)$$

and for $\tilde{\lambda} = 0.35$ a transversal homoclinic orbit $x_{\mathbb{Z}}(\tilde{\lambda})$ w.r.t. the fixed point $\xi_+(\tilde{\lambda})$ exists, satisfying Assumption **A4**.

For numerical computations, we approximate an infinite homoclinic orbit $x_{\mathbb{Z}}(\tilde{\lambda})$ by a finite orbit segment x_J, where $J = [n_-, n_+] \cap \mathbb{Z}$. The segment is determined as a zero of the boundary value operator

$$\Gamma_J(x_J, \tilde{\lambda}) = \begin{pmatrix} x_{n+1} - f(x_n, \tilde{\lambda}), & n = n_-, \dots, n_+ - 1 \\ b(x_{n_-}, x_{n_+}) \end{pmatrix}.$$

Here $b : \mathbb{R}^{2k} \to \mathbb{R}^k$ defines a boundary condition, for example

$$b_{\text{per}}(x,y) = x - y, \quad \text{or} \quad b_{\text{proj}}(x,y) = \begin{pmatrix} B_s(x - \bar{\xi}) \\ B_u(x - \bar{\xi}) \end{pmatrix},$$

in case of periodic and projection boundary conditions, where B_s and B_u yield linear approximations of the stable and the unstable manifold. Due to our hyperbolicity assumption, $\Gamma_J(\cdot, \tilde{\lambda})$ has for J sufficiently large a unique zero in a neighborhood of the exact solution. Moreover approximation errors decay at an exponential rate that depends on the type of boundary condition, cf. [4].

For Hénon's map, we solve the corresponding boundary value problem, obtain in this way an approximation of $x_{\mathbb{Z}}(\tilde{\lambda})$ and continue this orbit w.r.t. the parameter λ, using the method of pseudo arclength continuation, cf. [25, 1, 17, 13]. In Figure 1, we plot the amplitude of these orbits $\text{amp}(x_J(\lambda)) := \left(\sum_{n\in J} \|x_n(\lambda) - \xi_+(\lambda)\|^2\right)^{\frac{1}{2}}$ versus the parameter. This figure is well known, cf. [4], but is reproduced here to illustrate and introduce our labeling of left and right turning points.

At the value $\tilde{\lambda} = 0.35$ four distinct homoclinic orbits occur that we denote by $x^i_{\mathbb{Z}}$, $i \in \{0, \dots, 3\}$. We choose their index by following the order given by the continuation routine. The orbit $x^0_{\mathbb{Z}}$ is shown in Figure 2 together with parts of the stable and the unstable manifold of the fixed point $\xi_+(\tilde{\lambda})$. The enlargements in the figure show which intersection of the manifolds leads to the four homoclinic orbits.

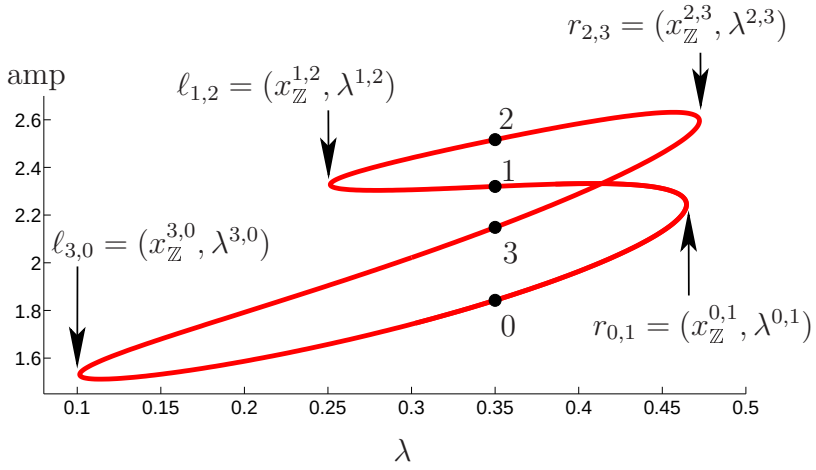

Figure 1: *Continuation of homoclinic Hénon orbits. At the parameter* $\tilde{\lambda} = 0.35$ *four distinct orbits* $x_{\mathbb{Z}}^i$, $i \in \{0, \dots, 3\}$ *exist that turn into each other via left or right turning points.*

At each turning point, two orbits collide; with r and ℓ, we distinguish right and left turning points. Figure 3 illustrates intersections of stable and unstable manifolds at these four turning points.

Errors of turning point calculations for finite approximations of homoclinic orbits decay exponentially fast w.r.t. the length of the computed orbit segment, cf. [27, Theorem 5.1.1]. We refer to [12], for algorithms that compute approximations of one-dimensional and two-dimensional stable and unstable manifolds and to [30] for a comparison of competing methods.

4 Connected components of multi-humped orbits

For Hénon's map, we find four distinct transversal homoclinic orbits $x_{\mathbb{Z}}^s$, $s \in \{0, \dots, 3\}$ at $\tilde{\lambda} = 0.35$ and we identify $x_{\mathbb{Z}}(s)$ with its symbol s. Note that the orbits $0, 1, 2, 3, 0$ pass into each other via left (L) and right (R) turning points $r_{0,1}$, $\ell_{1,2}$, $r_{2,3}$, $\ell_{3,0}$, see Figure 3. The graph in Figure 4 gives an alternative illustration of these transitions.

The transition graph for one-humped orbits in Figure 4 consists of exactly one LR-cycle. Note that all one-humped orbits lie on a single closed curve and thus are found via numerical continuation.

The corresponding analysis of closed curves of n-humped orbits, with $n \geq 2$, is more involved and is the main goal of this section. Indeed, several disjoint curves of n-humped orbits occur. We introduce a symbolic coding for n-humped

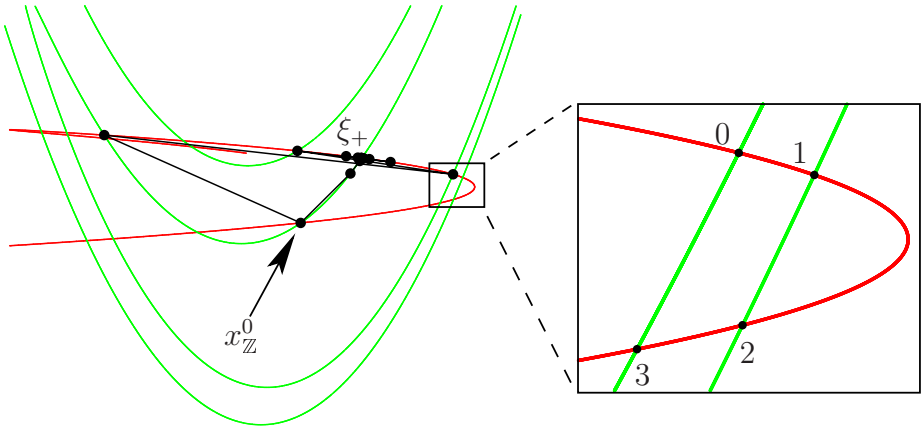

Figure 2: *Primary homoclinic orbit $x^0_{\mathbb{Z}}$ w.r.t. the fixed point ξ_+, and parts of the stable manifold (green) and the unstable manifold (red). The enlargement shows the intersections of manifolds that lead to the four homoclinic orbits in Figure 1.*

orbits and put two orbits into the same equivalence class, if they lie on the same closed curve.

For the construction of an n-humped orbit, we choose a sufficiently long interval $J = [n_-, n_+]$ around zero and a sequence $s \in \mathcal{S}^n := \{0, \dots, 3\}^n$. We define the pseudo orbit

$$\tilde{x}_{\mathbb{Z}}[s] := x^{s_1}_{(-\infty, n_+]} x^{s_2}_J \dots x^{s_{n-1}}_J x^{s_n}_{[n_-, \infty)}, \tag{4.1}$$

see Figure 5. Since the collection of single orbits $x^r_{\mathbb{Z}}$, $r \in \{0, \dots, 3\}$ together with the fixed point forms a hyperbolic set, the Shadowing-Lemma, cf. [38, 36] shows that the pseudo orbit $\tilde{x}_{\mathbb{Z}}(s)$ lies close to a true n-humped f-orbit which we denote by $x_{\mathbb{Z}}(s)$. In $\mathcal{S}^n$ there are 4^n different symbols and thus we expect to find 4^n different n-humped orbits $x_{\mathbb{Z}}(s)$. We identify these orbits with their symbol. Note that composing initial approximations of multi-humped orbits from pieces of single orbits is a very common approach that appears in discrete as well as continuous time dynamical systems, see [8, 31, 29, 34].

We also note that our construction of pseudo orbits in (4.1) slightly differs from (2.11), where we add up shifted orbits. With both approaches, we expect to find the same shadowing orbit for sufficiently large intervals J.

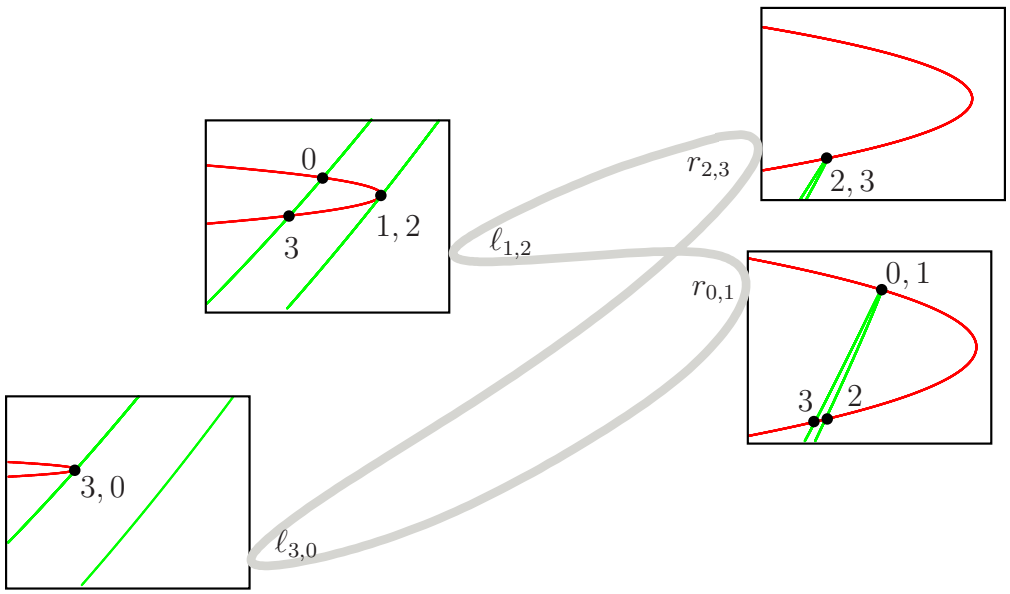

Figure 3: *Intersections of stable and unstable manifolds at the four turning points in the cutout region from Figure 2.*

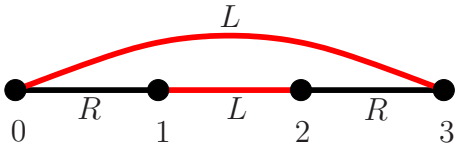

Figure 4: *Transition graph for one-humped orbits.*

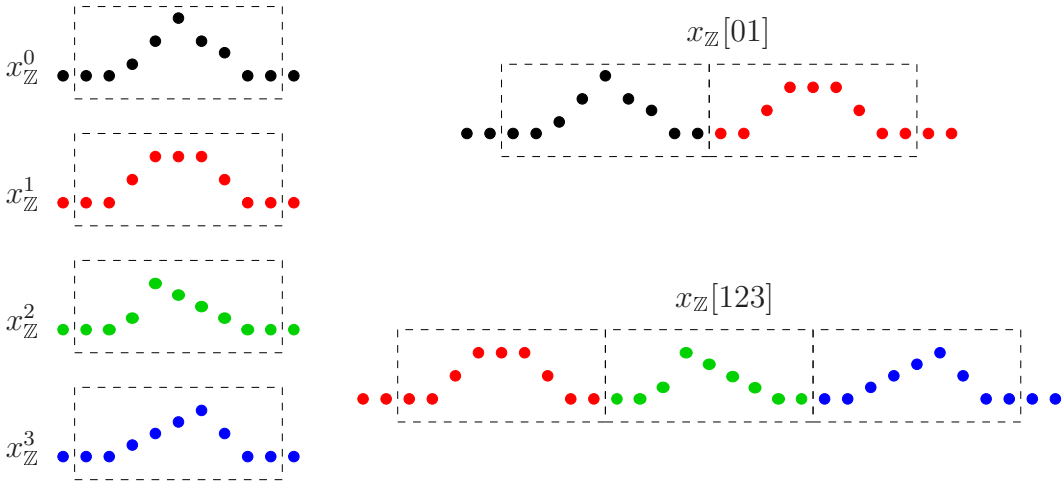

Figure 5: *Construction of multi-humped orbits.*

Given two symbols $s, \bar{s} \in \mathcal{S}^n$, we analyze whether the n-humped orbits $x_{\mathbb{Z}}(s)$ and $x_{\mathbb{Z}}(\bar{s})$ can turn into each other via continuation.

Let us first look at the two-humped case.

4.1 Bifurcation of two-humped orbits

The continuation of two-humped orbits exhibits three closed curves of homoclinic orbits, see Figure 6. At the parameter value $\tilde{\lambda}$, there exist 16 different homoclinic orbits $x_{\mathbb{Z}}(s)$, indexed by $s \in \mathcal{S}^2$. These orbits lie on different closed curves, namely 8 on the first, and 4 on the second and the third curve.

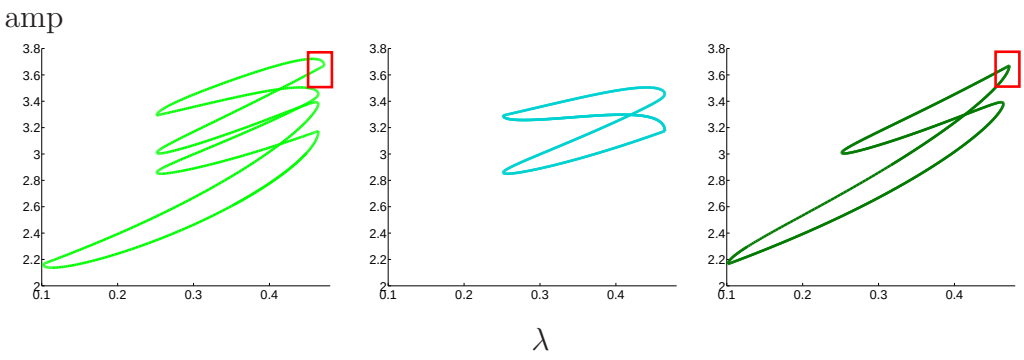

Figure 6: *Continuation of two-humped orbits of length* $n_- = -20$, $n_+ = 21$.

We note that it is challenging to compute the continuation pictures in Figure 6 due to the sharp turns that occur, see Figure 7.

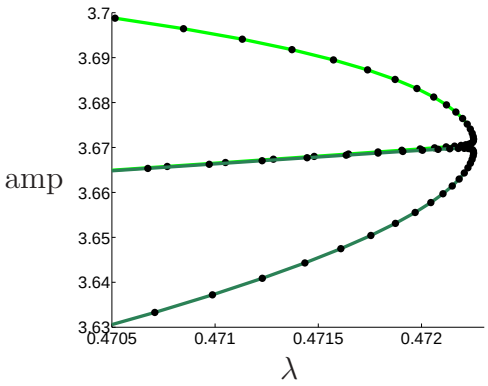

Figure 7: *Zoom of the red box in Figure 6, showing sharp turns of curves of* 2*-humped orbits. The black points are computed by our continuation routine and illustrate the decrease of step sizes.*

An accurate step size control is essential for achieving these diagrams. With too large continuation steps, the algorithm directly jumps from the upper light green to the lower dark green curve.

For the continuation of n-humped orbits, this problem also shows up with available software like MATCONT, cf. [13], when using the standard setup of parameters. We therefore apply our own implementation of an Euler-Newton method which controls the step size by $\mathrm{cond}^{-\alpha}$, where $\alpha \in [0.7, 0.81]$ and cond denotes the condition number of the Jacobian, occurring in the Newton process of the corrector step. The difficulty of continuing n-humped orbits across the sharp turns is illustrated by the minimal step sizes that we find during the computation, see Table 1.

n	2	3	4	5
$h_{\min}$	$9 \cdot 10^{-4}$	$8 \cdot 10^{-6}$	$9 \cdot 10^{-7}$	$2 \cdot 10^{-7}$

Table 1: *Minimal step sizes $h_{\min}$ of our algorithm for the continuation of n-humped orbits.*

The following discussion explains why a large condition number close to the sharp turns is to be expected.

One observes that at each turning point in Figure 6, exactly one component of the symbol changes. For example, the symbol $(1, 1)$ changes at a left turning point into the symbol $(2, 1)$. But why does the symbol $(1, 1)$ not change into the symbol $(1, 2)$? The answer, which transition occurs depends on small terms that perturb a hilltop bifurcation, see the discussion below. These small terms are caused by the finite distance between the single humps.

For two-humped orbits, the system (2.23) is a set of two equations in three variables λ, τ_1, τ_2, called the hilltop normal form, cf. [14]

$$\lambda = \tau_1^2, \quad \lambda = \tau_2^2. \tag{4.2}$$

Figure 8 (left) shows the solution curves of (4.2) while the red curves in Figure 8 (right) indicate the generic solution picture of a perturbed equation. Here we neglect more detailed bifurcation diagrams which take into account small hysteresis effects w.r.t. the parameter λ, see [14, Ch. IX, §3] for the unfolding theory.

Note that the Jacobian of the Newton process becomes singular at a simple bifurcation point, cf. [10], and hence is ill-conditioned at a perturbed bifurcation.

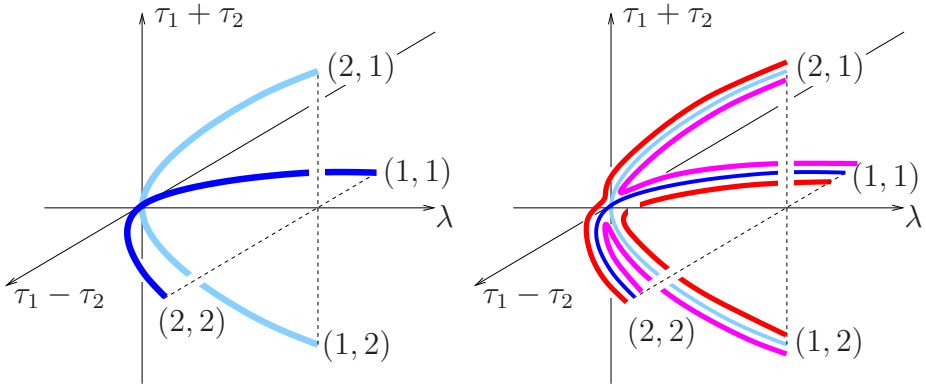

Figure 8: *Unperturbed (left) and perturbed hilltop bifurcation (right) at the turning point* $\ell_{1,2}$.

4.2 Connected components and equivalent symbols

Homoclinic orbits that lie on a common closed curve define a connected component of

$$\mathcal{H} := \big\{(y_{\mathbb{Z}},\lambda) \in \ell^\infty(\mathbb{R}^k)\times\mathbb{R} : y_{n+1} = f(y_n,\lambda)\ \forall n\in\mathbb{Z},\ \lim_{n\to\pm\infty} y_n = \xi(\lambda)\big\}.$$

More precisely, let $s \in \mathcal{S}^n$ and denote by $C(s) \subset \mathcal{H}$ the connected component that satisfies $(x_{\mathbb{Z}}(s),\tilde{\lambda}) \in C(s)$.

Then, we obtain an equivalence relation by identifying two sequences $s,\bar{s} \in \mathcal{S}^n$, if the corresponding orbits lie in the same component i.e.

$$s \cong \bar{s} \quad\Leftrightarrow\quad (x_{\mathbb{Z}}(\bar{s}),\tilde{\lambda}) \in C(s). \tag{4.3}$$

In the following, we discuss how to find these equivalence classes. In particular, we show under some generic assumptions that each equivalence class has at least four elements, and for n-humped orbits it turns out that one class has at least $4n$ elements.

For this task, we introduce a labeled graph G with vertices $s \in \mathcal{S}^n$. Two vertices s and $\bar{s} \in \mathcal{S}^n$ are connected with an L or R-edge, if $x_{\mathbb{Z}}(s)$ bifurcates into $x_{\mathbb{Z}}(\bar{s})$ via a left or right turning point. Since we do not know the effect of the perturbed hilltop bifurcation a priori, we put an edge, if the transition is possible for at least one perturbation. For example, the vertices $(1,1)$ and $(2,1)$ as well as $(1,1)$ and $(1,2)$ are connected with L-edges in case $n=2$, see Section 4.1. Precise rules for constructing this graph are stated in Section 4.3.

Our hypothesis is that the desired equivalence classes correspond to *a special* decomposition of this graph into disjoint LR-cycles.

In case of one-humped orbits, the only LR-cycle is 01230, see Figure 4. Consequently, all symbols lie in the same equivalence class, which matches the fact

that all one-humped orbits lie on the same closed curve and thus, in the same connected component of $\mathcal{H}$.

4.3 Graph structure of homoclinic network

In this section, we give precise rules for defining the labeled graph G which we identify with its adjacency tensor with entries R and L.

First, we assume that only one of the n humps can turn into a neighboring hump at a turning point.

R1 There is no edge from $s \in \mathcal{S}^n$ to $\bar{s} \in \mathcal{S}^n$ if

$$s = \bar{s} \quad \text{or} \quad \|s - \bar{s}\|_1 = \sum_{i=1}^{n} d(s_i, \bar{s}_i) \geq 2,$$

where d is the distance on the cycle 01230.

Now let $s, \bar{s} \in \mathcal{S}^n$ and assume $\|s - \bar{s}\|_1 = 1$, then there exists a unique j such that $s_j \neq \bar{s}_j$.

From $\lambda^{2,3} > \lambda^{0,1}$ we conclude that the right transition at $r_{2,3}$ can only occur if the orbit contains no 0 and no 1 hump. Therefore, we define R-edges in G according to the following rule.

R2 $G(s, \bar{s}) = R$ if

- $\{s_j, \bar{s}_j\} = \{0, 1\}$,
- $\{s_j, \bar{s}_j\} = \{2, 3\}$ and $s_i \in \{2, 3\}$ for all $i = 1, \ldots, n$.

Similarly from $\lambda^{1,2} > \lambda^{3,0}$ we conclude that the left transition at $\ell_{3,0}$ can only occur if the orbit contains no 1 and no 2 hump. Our rules for L-edges are:

R3 $G(s, \bar{s}) = L$ if

- $\{s_j, \bar{s}_j\} = \{1, 2\}$,
- $\{s_j, \bar{s}_j\} = \{0, 3\}$ and $s_i \in \{0, 3\}$ for all $i = 1, \ldots, n$.

We expect a connected component to correspond to an LR-cycle in this graph, i.e. a cycle on which L and R-edges alternate. A precise statement of our hypothesis is as follows.

Hypothesis 8 *The connected components of n-humped orbits and thus the equivalence classes* (4.3) *are in one to one correspondence to partitions of G into disjoint LR-cycles.*

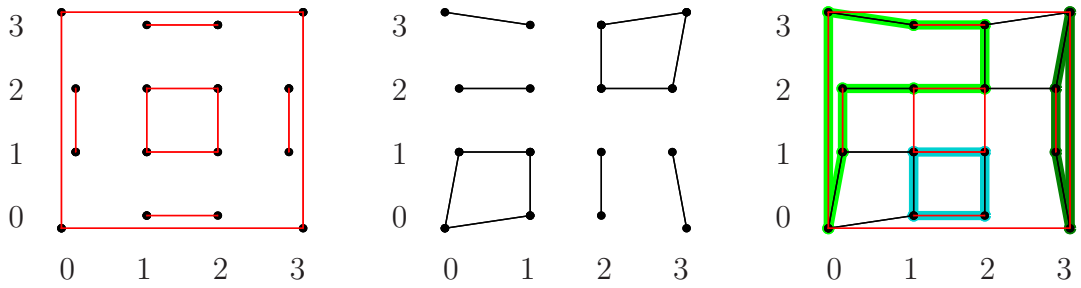

Figure 9: *L-edges of G (left) and R-edges (center) for two-humped orbits. The cycles in the right figure correspond to the closed curves that are computed numerically in Figure 6.*

In case $n = 2$, the L and R-edges are shown in the left and center picture of Figure 9, respectively. The right diagram additionally shows the LR-cycles that correspond to the connected components from Figure 6.

A partition of the graph into disjoint LR-cycles is not unique and consequently, the decomposition in the right of Figure 9 is not the only possible candidate, satisfying Hypothesis 8. Figure 10 illustrates all possible partitions (up to reflections at the diagonal).

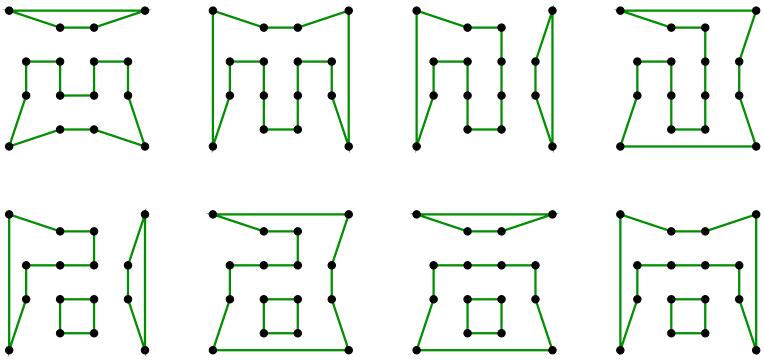

Figure 10: *All possible decompositions (up to symmetry) into disjoint LR-cycles.*

Our numerical results show that the first partition in the second row of Figure 10 actually occurs in the Hénon system. This indicates the particular paths (red or magenta in Figure 8) taken on each perturbed hilltop bifurcation.

Corresponding diagrams for $n = 3$ are given in Figure 11.

We continued n-humped orbits numerically for Hénon's map up to $n = 5$. Table 2 summarizes the number of cycles and their lengths found in the computation.

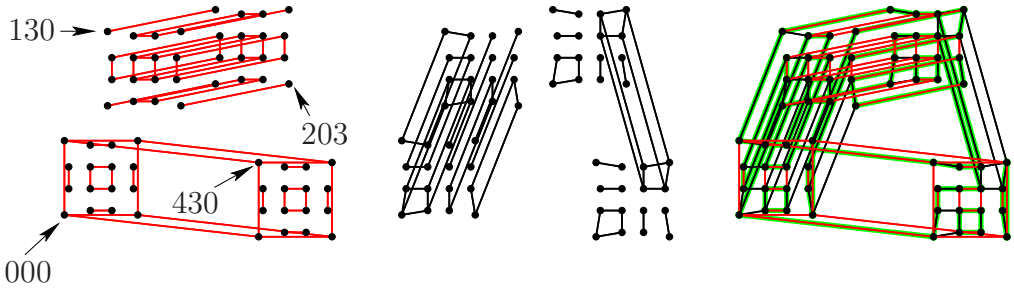

Figure 11: *L-edges of G (left) and R-edges (center) for three-humped orbits. The green lines in the right figure show the cycles that are computed numerically.*

	length of cycle				
n	4	8	12	16	20
1	1				
2	2	1			
3	9	2	1		
4	45	3	3	1	
5	205	6	6	4	1

Table 2: *Continuation of n-humped orbits – length of occurring cycles in numerical experiments.*

Hypothesis 8 relates connected components of $\mathcal{H}$ to LR-cycles in the graph G, given by our rules **R1-R3**. Even though we cannot decompose G uniquely into disjoint LR-cycles, our experiments for n-humped orbits of Hénon's map suggest that the length of occurring cycles is always a multiple of 4. Furthermore, there exists one cycle of length at least $4n$. Indeed, we prove that these observations follow from Hypothesis 8.

Theorem 9 *Fix $n \in \mathbb{N}$ and assume that Hypothesis 8 holds true. Then, all n-humped orbits lie on cycles whose length is a multiple of 4.*

For the specific symbols $s^0 = (0, \ldots, 0)$ and $s^2 = (2, \ldots, 2) \in \mathcal{S}^n$, the corresponding orbits $x_{\mathbb{Z}}(s^0)$ and $x_{\mathbb{Z}}(s^2)$ lie on a common cycle of at least length $4n$.

Remark 10 *Table 2 shows that there is exactly one orbit of length $4n$ and all other orbits are shorter. Hence, the orbit of length $4n$ contains s^0 and s^2.*

Proof: By assuming Hypothesis 8 we see that it suffices to analyze LR-cycles of the graph G. More precisely, we prove Theorem 9 along the following steps.

(i) Each LR-cycle in G has length $4m$, $m \geq 1$, $m \in \mathbb{N}$.

(ii) There exists an LR-cycle from s^0 to s^2 of length $4n$ and each LR-cycle that contains s^0 and s^2 has at least length $4n$.

(iii) Each LR-cycle that contains s^0 also contains s^2.

(i) Let the vertices $v^1, \dots, v^m, v^{m+1} = v^1$ form an LR-cycle in G. Fix $j \in \{1, \dots, n\}$ and let $l_j = \#\big\{i \in \{1, \dots, m\} : v^i_j \neq v^{i+1}_j,\ G(v^i, v^{i+1}) = L\big\}$ be the number of L-edges for which the corresponding vertices only differ in the jth component.

From **R1** it follows that l_j is an even number and $\max_{j=1,\dots,n}\{l_j\} \geq 2$, otherwise the cycle cannot be closed in the jth component. Furthermore, an LR-cycle has the same number of L and R-edges. Thus, the cycle has length

$$m = \sum_{i=1}^{n} 2l_i = 4\sum_{i=1}^{n} \frac{l_i}{2} = 4p \quad \text{with} \quad p = \sum_{i=1}^{n} \frac{l_i}{2} \geq 1.$$

(ii) We explicitly construct an LR-cycle in G from s^0 to s^2: $(0\cdots0) \mapsto (10\cdots0) \mapsto (20\cdots0) \mapsto (210\cdots0) \mapsto (220\cdots0) \mapsto \cdots \mapsto (2\cdots2) \mapsto (32\cdots2) \mapsto (312\cdots2) \mapsto (302\cdots2) \mapsto (3012\cdots2) \mapsto (3002\cdots2) \mapsto (30\cdots0) \mapsto (0\cdots0)$ which has length $4n$. Note that the distance from s^0 to s^2 on the full quadratic grid is $2n$ and consequently, each cycle containing these two points has at least length $4n$.

(iii) For proving that each LR-cycle with s^0 also contains s^2, assume that an LR-cycle exists that contains s^2 but not s^0. This cycle lies in the subgraph that we obtain by deleting the vertex s^0 with its corresponding edges.

Note that the LR-cycles start with an L and end with an R-edge, and it follows from **R2** that all R-edges that start at s^2 end in

$$V_3 := \{s \in \mathcal{S}^n :\ \exists j \in \{1, \dots, n\} :\ s_j = 3\}.$$

We define the graph $\tilde{G}$ by deleting the R-edges of s^2 from the remaining graph. Figure 12 illustrates this construction in case $n = 2$.

If $\tilde{G}$ breaks into two components V_3 and $\tilde{G} \setminus V_3$, then we get a contradiction to the above assumption and an LR-cycle in the original graph G that contains s^2 but not s^0 cannot exist.

To finish the proof, we show that an LR-path in $\tilde{G}$ from s^2 to V_3 does not exist.

From s^2 we cannot go directly via an R-edge to V_3, since the corresponding edges are deleted in $\tilde{G}$. Thus without loss of generality, we get: $(2\cdots2) \mapsto (12\cdots2) \mapsto (02\cdots2)$. Denote by v^m the mth vertex on this path. A 3-component can only be achieved by the left transition $\ell_{3,0}$ or by the right transition $r_{2,3}$, see **R2** and **R3**.

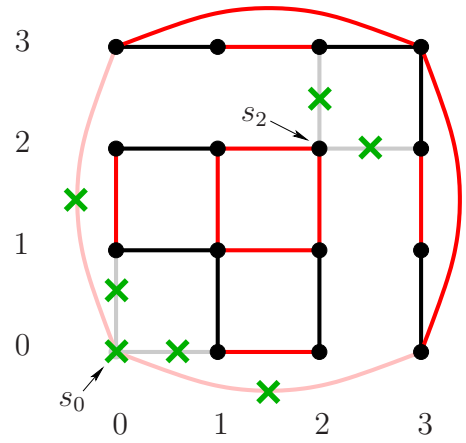

Figure 12: *Transition graph in case $n = 2$. L-edges and R-edges are plotted in red and black, respectively. Vertices and edges that are deleted in the proof of Theorem 9 are marked by green crosses.*

If a j exists with $v_j^m \in \{0, 1\}$, then the $r_{2,3}$ transition is impossible by **R2**.

If a j exists with $v_j^m \in \{1, 2\}$, then the $\ell_{3,0}$ transition is impossible by **R3**.

Thus, we only obtain a 3 component via the vertex $s^0 = (0 \dots 0)$ which is deleted in $\tilde{G}$.

■

In summary, 4^n different n-humped orbits for Hénons map exist at the parameter value $\tilde{\lambda} = 0.35$. These orbits share the same connected component, if they turn into each other via parameter-continuation. We have introduced a symbolic coding and proposed rules to decide a-priori, if two orbits lie on a common component. Via a graph theoretical argument, it turns out that the minimal component size is 4. Furthermore, the orbits coded by $(0 \cdots 0)$ and $(2 \cdots 2)$ lie on a common curve and this curve connects at least $4n$ orbits via continuation.

A complete classification of the 4^n orbits into connected components requires more knowledge on perturbations of hilltop bifurcations that we have not yet analyzed. We presented numerical data found for the cases of $2 - 5$-humped orbits.

5 Bifurcation analysis near homoclinic tangencies

In this section we prove the main Theorem 1 and Theorem 5(i) by using an existence and uniqueness result for a suitable operator equation in spaces of

bounded sequences. In the following we use the notation $B_\rho(x)$ and $B_\rho = B_\rho(0)$ to denote closed balls of radius ρ in some Banach space.

5.1 The operator equation

First recall the operator $F : \ell^\infty(\mathbb{R}^k) \times \mathbb{R} \to \ell^\infty(\mathbb{R}^k)$ from (2.19) and the normalization $\bar{\lambda} = 0$ and $\xi(\lambda) = 0$ for λ close to $\bar{\lambda}$, see **A2**, **A3** in Section 2. Then for any $s \in \Omega_N$ define the operator

$$G_s : \ell^\infty(\mathbb{R}^k) \times \ell^\infty(s) \times \ell^\infty(s) \times \mathbb{R} \to \ell^\infty(\mathbb{R}^k) \times \ell^\infty(s)$$

by

$$G_s(x_\mathbb{Z}, g, \tau, \lambda) = \begin{pmatrix} F(p_\mathbb{Z}(s) + x_\mathbb{Z} + v_\mathbb{Z}(s,\tau), \lambda) + w(s,g) \\ \langle \beta^{-\ell} u_\mathbb{Z}, x_\mathbb{Z} \rangle,\ \ell \in I(s) \end{pmatrix}. \tag{5.1}$$

Here $p_\mathbb{Z}$, $v_\mathbb{Z}$ are defined in (2.11), (2.13) and $w(s,g)$ is given by (recall $w_\mathbb{Z}$ from (2.16))

$$w(s,g) = \sum_{\ell \in I(s)} g_\ell \beta^{-\ell} w_\mathbb{Z}, \quad g \in \ell^\infty(s).$$

Our aim is to derive the functions $x_{\mathbb{Z},s}$, g_s in Theorem 1 by solving

$$G_s(x_\mathbb{Z}, g, \tau, \lambda) = 0 \tag{5.2}$$

for $\|\tau\|_\infty$, $|\lambda|$ sufficiently small and for all $s \in \Omega_N$. More precisely, we prove in Section 6 the following *Reduction Theorem.*

Theorem 11 *There exist constants $C_0, \rho_x, \rho_g, \rho_\tau, \rho_\lambda > 0$ and a number $N_0 \in \mathbb{N}$ such that for all $N \geq N_0$ and for all $s \in \Omega_N$ the following statements hold. For all $\tau \in B_{\rho_\tau}$, $\lambda \in B_{\rho_\lambda}$ the system (5.2) has a unique solution*

$$g = g_s(\tau, \lambda) \in B_{\rho_g} \subset \ell^\infty(s), \quad x_\mathbb{Z} = x_{\mathbb{Z},s}(\tau, \lambda) \in B_{\rho_x} \subset \ell^\infty(\mathbb{R}^k).$$

Moreover, the following estimate is satisfied:

$$\max(\|g - \tilde{g}\|_\infty, \|x_\mathbb{Z} - \tilde{x}_\mathbb{Z}\|_\infty) \leq C_0 \|G_s(x_\mathbb{Z}, g, \tau, \lambda) - G_s(\tilde{x}_\mathbb{Z}, \tilde{g}, \tau, \lambda)\| \tag{5.3}$$

for all $g, \tilde{g} \in B_{\rho_g}$, $x_\mathbb{Z}, \tilde{x}_\mathbb{Z} \in B_{\rho_x}$, $\tau \in B_{\rho_\tau}$, $\lambda \in B_{\rho_\lambda}$.

5.2 Preparatory Lemmata

In order to construct the neighborhoods U and Λ in Theorem 1 we need several lemmata.

Lemma 12 *There exists $N_1 \in \mathbb{N}$, such that for all $N \geq N_1$, $s \in \Omega_N$ the linear system*

$$\sum_{k\in I(s)} \langle \beta^{-\ell} u_{\mathbb{Z}}, \beta^{-k} u_{\mathbb{Z}} \rangle \tau_k = r_\ell, \quad \ell \in I(s),\ r \in \ell^\infty(s) \tag{5.4}$$

has a unique solution $\tau \in \ell^\infty(s)$ and

$$\|\tau\|_\infty \leq 2\|r\|_\infty. \tag{5.5}$$

Proof: Rewrite (5.4) as fixed point equation

$$\tau = P\tau + r, \quad (P\tau)_\ell = -\sum_{k\in I(s), k\neq\ell} \langle \beta^{-\ell} u_{\mathbb{Z}}, \beta^{-k} u_{\mathbb{Z}} \rangle \tau_k$$

and note

$$\begin{aligned} \|P\tau\|_\infty &\leq \|\tau\|_\infty \sup_{\ell\in I(s)} \sum_{k\in I(s), k\neq\ell} |\langle u_{\mathbb{Z}}, \beta^{\ell-k} u_{\mathbb{Z}} \rangle| \\ &\leq \|\tau\|_\infty C \sum_{j\geq 1} \mathrm{e}^{-\alpha j N} = \frac{C\mathrm{e}^{-\alpha N}}{1-\mathrm{e}^{-\alpha N}} \|\tau\|_\infty. \end{aligned}$$

Thus, we choose N_1 such that $\frac{C\mathrm{e}^{-\alpha N_1}}{1-\mathrm{e}^{-\alpha N_1}} \leq \frac{1}{2}$. Then P is contractive and (5.5) follows. ■

Lemma 13 *There exist $N_2 \in \mathbb{N}$, $C_2 > 0$ such that*

$$\|F(p_{\mathbb{Z}}(s) + v_{\mathbb{Z}}(s,\tau), \lambda)\|_\infty \leq C_2(|\lambda| + \|\tau\|_\infty^2 + \mathrm{e}^{-\alpha N/2}) \tag{5.6}$$

for all $N \geq N_2$, $s \in \Omega_N$, $|\lambda| \leq 1$, $\tau \in B_1 \subset \ell^\infty(s)$.

Proof: We estimate

$$\begin{aligned} & p_{n+1}(s) + v_{n+1}(s,\tau) - f(p_n(s) + v_n(s,\tau), \lambda) \\ = & \sum_{\ell\in I(s)} (\bar{x}_{n+1-\ell} + \tau_\ell u_{n+1-\ell}) - f(p_n(s) + v_n(s,\tau), 0) + \mathcal{O}(|\lambda|) \\ = & \sum_{\ell\in I(s)} \big(f(\bar{x}_{n-\ell}, 0) + \tau_\ell f_x(\bar{x}_{n-\ell}, 0) u_{n-\ell} \big) \\ & - f\big(\sum_{\ell\in I(s)} \bar{x}_{n-\ell} + \sum_{\ell\in I(s)} \tau_\ell u_{n-\ell}, 0 \big) + \mathcal{O}(|\lambda|) \\ = & \sum_{\ell\in I(s)} f(\bar{x}_{n-\ell}, 0) + \sum_{\ell\in I(s)} \tau_\ell f_x(\bar{x}_{n-\ell}, 0) u_{n-\ell} \\ & - f\big(\sum_{\ell\in I(s)} \bar{x}_{n-\ell}, 0 \big) - f_x\big(\sum_{j\in I(s)} \bar{x}_{n-j}, 0 \big) \sum_{\ell\in I(s)} \tau_\ell u_{n-\ell} + \mathcal{O}(|\lambda| + \|\tau\|_\infty^2). \end{aligned}$$

For $n \in \mathbb{Z}$, choose $\tilde{\ell} \in I(s)$ such that $|n - \tilde{\ell}| \leq |n - \ell|$ for all $\ell \in I(s)$. Then $|n - \ell| \geq \frac{N}{2}$ for all $\ell \neq \tilde{\ell}$ and, therefore, by (2.6),

$$\begin{aligned} & \Big\| \sum_{\ell \in I(s)} f(\bar{x}_{n-\ell}, 0) - f\big(\sum_{\ell \in I(s)} \bar{x}_{n-\ell}, 0\big) \Big\| \\ \leq \ & \Big\| \sum_{\ell \in I(s), \ell \neq \tilde{\ell}} f(\bar{x}_{n-\ell}, 0) \Big\| + \Big\| f(\bar{x}_{n-\tilde{\ell}}, 0) - f\big(\sum_{\ell \in I(s)} \bar{x}_{n-\ell}, 0\big) \Big\| \\ \leq \ & \Big\| \sum_{\ell \in I(s), \ell \neq \tilde{\ell}} \bar{x}_{n+1-\ell} \Big\| + L \Big\| \sum_{\ell \in I(s), \ell \neq \tilde{\ell}} \bar{x}_{n-\ell} \Big\| \leq C_2 \mathrm{e}^{-\alpha N/2}. \end{aligned} \tag{5.7}$$

In a similar way,

$$\sum_{\ell \in I(s)} \tau_\ell f_x\big(\sum_{j \in I(s)} \bar{x}_{n-j}, 0\big) u_{n-\ell} = \sum_{\ell \in I(s)} \tau_\ell f_x(\bar{x}_{n-\ell}, 0) u_{n-\ell} + \mathcal{O}(\mathrm{e}^{-\alpha N/2} \|\tau\|_\infty). \tag{5.8}$$

Combining these estimates, we obtain (5.6). ■

Lemma 14 *Assume **A1**, **A2** and let $\bar{x}_\mathbb{Z}$ be a homoclinic $f(\cdot, 0)$-orbit with respect to the hyperbolic fixed point 0. Then, there exist neighborhoods $U_3 \subset \mathbb{R}^k$ of 0, $\Lambda_3 \subset \Lambda_0$ and constants $N_3, n_0, \alpha > 0, C_3 \geq 1$ such that the following statement holds for all $K \geq N_3$, $-n_-, n_+ \geq n_0$:*

If $x_{n+1} = f(x_n, \lambda)$ for $n \in \tilde{J} := [0, K-1]$, $\lambda \in \Lambda_3$, and if $x_n \in U_3$ for all $n \in J := [0, K]$ then we have the estimate

$$\sup_{j \in J} \|x_j - \bar{x}_{n_- + 1 - K + j} - \bar{x}_{n_+ - 1 + j}\| \leq C_3 \left(\|x_K - \bar{x}_{n_- + 1}\| + \|x_0 - \bar{x}_{n_+ - 1}\| + |\lambda| + \mathrm{e}^{-\alpha \frac{K}{2}} \right).$$

Furthermore we obtain in case $K = \infty$:

$$\sup_{j \geq 0} \|x_j - \bar{x}_{n_+ - 1 + j}\| \leq C_3 (\|x_0 - \bar{x}_{n_+ - 1}\| + |\lambda|). \tag{5.9}$$

Proof: Consider the pseudo-orbit $p_j := \bar{x}_{n_+ - 1 + j} + \bar{x}_{n_- + 1 - K + j}$, $j \in J$ which is a zero of the boundary value operator

$$\Gamma_J(y_J, \lambda) := \begin{pmatrix} y_{n+1} - f(y_n, \lambda) - \rho_n, & n \in \tilde{J} \\ b_K(y_0, y_K) \end{pmatrix},$$

at $\lambda = 0$, where

$$\begin{aligned} \rho_n &:= f(\bar{x}_{n_+ - 1 + n}, 0) + f(\bar{x}_{n_- + 1 - K + n}, 0) - f(p_n, 0), \quad n \in J, \\ b_K(y_0, y_K) &:= \begin{pmatrix} P_s(y_0 - p_0) \\ P_u(y_K - p_K) \end{pmatrix}. \end{aligned}$$

Here P_s and P_u are the stable and unstable projectors of the fixed point 0.

Let b be the bound from Theorem 22 for the difference equation

$$u_{n+1} = (f_x(0,0) + B_n)u_n, \quad B_n = f_x(p_n, \lambda) - f_x(0,0), \quad n \in \tilde{J}.$$

For sufficiently large $-n_-, n_+ \geq n_0$ and $\lambda \in \Lambda_3$ sufficiently small, we get $\|B_n\| \leq b$ for all $n \in \tilde{J}$. Consequently

$$u_{n+1} = f_n(p_n, \lambda)u_n, \quad n \in \tilde{J}$$

has an exponential dichotomy on J with projectors P_n^s, P_n^u and an exponential rate α that is independent of n_-, n_+, λ and K.

As in the proof of [23, Theorem 4], we show that for $\lambda \in \Lambda_3$, $n_-, n_+ \geq n_0$ and $K \geq N_3$ we have a uniform bound

$$\|D_1\Gamma_J(p_J, \lambda)^{-1}\|_\infty \leq \sigma^{-1}. \tag{5.10}$$

In order to see this, consider the inhomogeneous difference equation

$$\begin{aligned} u_{n+1} - f_x(p_n, \lambda)u_n &= r_n, \quad n = 0, \dots K-1, & (5.11)\\ P_s u_0 + P_u u_K &= \gamma. & (5.12) \end{aligned}$$

Denote by Φ the solution operator of the homogeneous equation and let G be the corresponding Green's function, cf. (6.16). The general solution of (5.11) is given by

$$u_n = \Phi(n,0)v + \sum_{m \in \tilde{J}} G(n, m+1)r_m, \tag{5.13}$$

where

$$v = v_- + \Phi(0,K)v_+, \quad v_- \in \mathcal{R}(P_0^s), \quad v_+ \in \mathcal{R}(P_K^u).$$

Inserting (5.13) into (5.12), it remains to solve

$$P_s\big(v_- + \Phi(0,K)v_+\big) + P_u\big(\Phi(K,0)v_- + v_+\big) = R,$$

with

$$R = \gamma - P_s \sum_{m \in \tilde{J}} G(0, m+1)r_m - P_u \sum_{m \in \tilde{J}} G(K, m+1)r_m.$$

This finite-dimensional system has a unique solution for $K \geq N_3$ sufficiently large since $\|P_s - P_0^s\| \to 0$ and $\|P_u - P_K^u\| \to 0$ as $K \to \infty$. Therefore, the system (5.11), (5.12) also has a unique solution u_J for K large and the dichotomy estimates lead to a bound

$$\|u_J\|_\infty \leq \sigma^{-1}(|\gamma| + \|r_J\|_\infty),$$

i.e. (5.10) holds.

We apply Theorem 20 with the space $Y = \ell^\infty_J = \{(y_n)_{n\in J} : y_n \in \mathbb{R}^k\}$ of finite sequences and with $Z = \ell^\infty_{\tilde J} \times \mathbb{R}^k$, both endowed with the sup-norm. We take $y_0 = p_J$ and use uniform data for all $\lambda \in \Lambda_3$. For δ sufficiently small we have

$$\|D_1\Gamma_J(x_J,\lambda) - D_1\Gamma_J(p_J,\lambda)\|_\infty \le \frac{\sigma}{2} \text{ for all sequences } x_J \in B_\delta(p_J), \lambda \in \Lambda_3,$$

and by choosing the neighborhood Λ_3 sufficiently small we get

$$\begin{aligned}
\|\Gamma_J(p_J,\lambda)\|_\infty &= \sup_{n\in\tilde J} \|p_{n+1} - f(p_n,\lambda) - \rho_n\| + \|b_K(p_0,p_K)\| \\
&= \sup_{n\in\tilde J} \|p_{n+1} - f(p_n,\lambda) + f(p_n,0) \\
&\qquad\qquad -f(\bar x_{n_+-1+n},0) - f(\bar x_{n_-+1-K+n},0)\| \\
&= \sup_{n\in\tilde J} \|f(p_n,0) - f(p_n,\lambda)\| \le \frac{\sigma}{2}\delta \quad \text{for } \lambda \in \Lambda_3.
\end{aligned}$$

Theorem 20 applies to $\lambda \in \Lambda_3$ with uniform data, and it follows from (A.5) with some constant $C_3 > 0$ that

$$\|x_J - y_J\|_\infty \le C_3\|\Gamma_J(x_J,\lambda) - \Gamma_J(y_J,\lambda)\|_\infty \quad \text{for all } x_J, y_J \in B_\delta(p_J), \lambda \in \Lambda_3. \tag{5.14}$$

From (2.6) we find a number n_0 such that $\bar x_n \in B_{\frac{\delta}{2}}(0)$ for all $|n| \ge n_0$ and also $p_n \in B_{\frac{\delta}{2}}(0), n \in J$ for all $-n_-, n_+ \ge n_0$. Then we take $U_3 := B_{\frac{\delta}{2}}(0)$ as our neighborhood and note that (5.14) holds for any two sequences x_J, y_J in U_3. For $n \in \tilde J$ and $\lambda \in \Lambda_3$ it follows that

$$\begin{aligned}
& f(p_n,\lambda) - p_{n+1} \\
= \;& f(\bar x_{n_+-1+n} + \bar x_{n_-+1-K+n},\lambda) - \bar x_{n_+-1+n+1} - \bar x_{n_-+1-K+n+1} \\
= \;& f(\bar x_{n_+-1+n} + \bar x_{n_-+1-K+n},0) - f(\bar x_{n_+-1+n},0) - f(\bar x_{n_-+1-K+n},0) + \mathcal{O}(|\lambda|) \\
= \;& \left\{ \begin{array}{ll} -f(\bar x_{n_-+1-K+n},0) + \mathcal{O}(\|\bar x_{n_-+1-K+n}\|) & \text{for } 0 \le n \le \frac{K}{2} \\ -f(\bar x_{n_+-1+n},0) + \mathcal{O}(\|\bar x_{n_+-1+n}\|) & \text{for } \frac{K}{2} < n \le K \end{array} \right\} + \mathcal{O}(|\lambda|) \\
= \;& \mathcal{O}(\mathrm{e}^{-\alpha\frac{K}{2}} + |\lambda|).
\end{aligned}$$

Now let x_J be a sequence in U_3 such that $x_{n+1} = f(x_n,\lambda)$ for all $n \in \tilde J$, and some $\lambda \in \Lambda_3$. Then

$$\begin{aligned}
\|x_J - p_J\|_\infty &\le C\|\Gamma_J(x_J,\lambda) - \Gamma_J(p_J,\lambda)\|_\infty \\
&\le C\Big(\sup_{n\in\tilde J}\|f(p_n,\lambda) - p_{n+1}\| + \|b_K(x_0,x_K)\|\Big) \\
&\le C\left(\mathrm{e}^{-\alpha\frac{K}{2}} + |\lambda| + \left\|\begin{pmatrix} P_s(x_0-p_0) \\ P_u(x_K-p_K)\end{pmatrix}\right\|\right) \\
&\le C\left(\mathrm{e}^{-\alpha\frac{K}{2}} + \|x_0-p_0\| + \|x_K-p_K\| + |\lambda|\right) \\
&\le C_3\left(\mathrm{e}^{-\alpha\frac{K}{2}} + \|x_0-\bar x_{n_+-1}\| + \|x_K-\bar x_{n_-+1}\| + |\lambda|\right).
\end{aligned}$$

In case $K = \infty$, one uses the operator

$$\tilde{\Gamma}_{\mathbb{N}}(y_{\mathbb{N}}, \lambda) = \begin{pmatrix} y_{n+1} - f(y_n), & n \in \mathbb{N} \\ P_s(y_0 - \bar{x}_{n_+-1}) \end{pmatrix},$$

and it turns out that $D_1\tilde{\Gamma}_{\mathbb{N}}(p_{\mathbb{N}}, \lambda)$ with $p_j = \bar{x}_{n_+-1+j}$ has a uniformly bounded inverse for $\lambda \in \Lambda_3$ and sufficiently large $-n_-,\ n_+$. Then the estimate (5.9) follows immediately.

■

5.3 Proof of Main Theorem

Let us first prove assertion (i) in Theorem 1.

Step 1: (Construction of neighborhoods U, Λ)

In the following $\Lambda_1 \supset \Lambda_2 \supset \dots$ will denote shrinking neighborhoods of 0. Let $\rho_g, \rho_x > 0$ be given by Theorem 11 and note that we can decrease ρ_τ, ρ_λ without changing the assertion of Theorem 11. Introduce the constants (cf. (2.6) and Lemma 13, 14)

$$\alpha_* = \mathrm{e}^{-\alpha}, \quad C_4 = C_3 + \frac{2C_e}{1-\alpha_*}, \quad C_5 = C_e\frac{3-\alpha_*}{1-\alpha_*}, \quad C_6 = C_0C_2 + \frac{2C_e}{1-\alpha_*}. \tag{5.15}$$

Let $\rho_\tau > 0$ be such that

$$C_5\rho_\tau \le \frac{\rho_x}{4}. \tag{5.16}$$

By Lemma 14 we can choose a ball $B_{3\varepsilon_0} \subset U_3$ and numbers $n_+, -n_- \ge n_0$ such that $\bar{x}_n \in B_{\varepsilon_0}$ for all $n \ge n_+ - 1$ and $n \le n_- + 1$. It is well known that the only full orbit in a small neighborhood of a hyperbolic fixed point is the fixed point itself (this follows from [41, Theorem III.7]). That is, we can assume w.l.o.g. that U_3, Λ_3 satisfy

$$y_{n+1} = f(y_n, \lambda),\ y_n \in U_3 (n \in \mathbb{Z}),\ \lambda \in \Lambda_3 \Rightarrow y_n = 0 \text{ for all } n \in \mathbb{Z}. \tag{5.17}$$

The set $\mathcal{K} = \{0\} \cup \{\bar{x}_n : n \le n_- \text{ or } n \ge n_+\}$ is compact and satisfies

$$f(\mathcal{K}, 0) \subset \mathcal{K} \cup \{\bar{x}_{n_-+1}\}.$$

Thus we find an $\varepsilon \le \varepsilon_0$ and $\Lambda_4 \subset \Lambda_3$ such that the following properties hold

$$V_0 := B_\varepsilon \cup \bigcup_{n\le n_-, n\ge n_+} B_\varepsilon(\bar{x}_n) \subset B_{2\varepsilon_0} \subset U_3, \tag{5.18}$$

the balls

$$B_j := B_\varepsilon(\bar{x}_{n_-+j}),\ j = 1, \dots, \varkappa := n_+ - 1 - n_- \tag{5.19}$$

are mutually disjoint,

$$f(V_0, \Lambda_4) \cap B_j = \emptyset \quad \text{for} \quad j = 2, \dots, \varkappa, \tag{5.20}$$

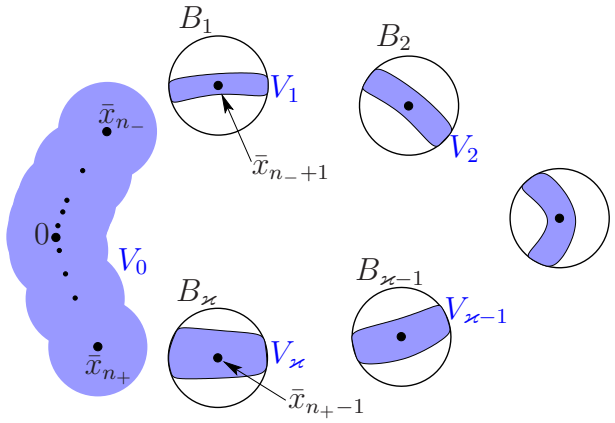

Figure 13: *Construction of neighborhoods.*

$$2C_5(2C_3+1)\varepsilon \le \frac{\rho_\tau}{3} \quad \text{and} \quad (2C_3+1)\varepsilon \le \frac{\rho_x}{4}, \tag{5.21}$$

see Figure 13.

Next we take $N_4 \ge \max(N_1, N_2, N_3)$ (see Lemmata 12, 13, 14) such that

$$2C_5C_4\mathrm{e}^{-\alpha N_4} \le \frac{\rho_\tau}{3}, \quad C_4\mathrm{e}^{-\alpha N_4} \le \frac{\rho_x}{4}, \quad (2(C_e+C_3)+18C_3C_6)\mathrm{e}^{-\alpha N_4} \le \frac{\varepsilon}{3}. \tag{5.22}$$

We can also find $\Lambda_5 \subset \Lambda_4$ such that for all $\lambda \in \Lambda_5$

$$2C_5C_3|\lambda| \le \frac{\rho_\tau}{3}, \quad C_3|\lambda| \le \frac{\rho_x}{4}, \quad |\lambda| \le \rho_\lambda, \quad 6C_3|\lambda|(3C_0C_2+1) \le \varepsilon. \tag{5.23}$$

Finally, we define

$$N = \varkappa + N_*, \quad \text{where} \quad N_* = 2N_4. \tag{5.24}$$

Then we choose $\Lambda_6 \subset \Lambda_5$ such that the following settings define neighborhoods V_j of $\bar{x}_{n_-+j}, j = \varkappa, \dots, 1$ recursively (cf. Figure 13):

$$\begin{aligned} V_\varkappa &= B_\varkappa \cap \bigcap_{n=1}^{N_*+1} f^{-n}(V_0, \Lambda_6), \\ V_j &= B_j \cap f^{-1}(V_{j+1}, \Lambda_6), \quad \text{for} \quad j = \varkappa-1, \dots, 1. \end{aligned} \tag{5.25}$$

Here we use the notation $f^{-n}(V_j, \Lambda_6) = \{x : f^n(x,\lambda) \in V_j \text{ for all } \lambda \in \Lambda_6\}$.

With these settings we consider the maximal invariant set $M(U,\Lambda)$, cf. (2.2), that belongs to

$$U = \bigcup_{j=0}^{\varkappa} V_j, \quad \Lambda = \Lambda_6. \tag{5.26}$$

Let us note that our construction (5.19), (5.20), (5.25), (5.26) implies the following three assertions for any $f(\cdot,\lambda)$-orbit $y_\mathbb{Z} \subset U$, $\lambda \in \Lambda$

$$y_n \in V_0, y_{n+1} \notin V_0 \Rightarrow y_{n+1} \in V_1, \tag{5.27}$$

$$y_n \in V_j \quad \text{for some} \quad 1 \le j \le \varkappa - 1 \Rightarrow y_{n+1} \in V_{j+1}, \tag{5.28}$$

$$y_n \in V_\varkappa \Rightarrow y_{n+\ell} \in V_0 \quad \text{for} \quad \ell = 1, \dots, N_* + 1. \tag{5.29}$$

Step 2:(Construction of symbolic sequence s)
For some $\lambda \in \Lambda$ consider an orbit $y_{\mathbb{Z}}$ of (1.1) that lies in U. If it lies in V_0 then $y_n = 0, n \in \mathbb{Z}$ by (5.17) and we set $s = 0 \in \Omega_N$. Otherwise we have $y_{\tilde{n}} \notin V_0$ for some $\tilde{n} \in \mathbb{Z}$. We show that

$$\tilde{I}(y_{\mathbb{Z}}) := \{n \in \mathbb{Z} : y_n \in V_1\}$$

is nonempty and that there is a unique $s \in \Omega_N$ such that $\tilde{I}(y_{\mathbb{Z}}) = I(s)$, see (2.8). By our assumptions we have $y_{\tilde{n}} \in V_{j_0}$ for some $j_0 \in \{1, \dots, \varkappa\}$. If $j_0 = 1$ then $\tilde{I}(y_{\mathbb{Z}}) \neq \emptyset$ whereas in case $j_0 \ge 2$ we obtain $y_{\tilde{n}-m} \in V_{j_0-m}, m = 0, \dots, j_0 - 1$ by induction from (5.28) and the fact that the V_j are mutually disjoint. Therefore, we have $\tilde{\ell} := \tilde{n} - j_0 + 1 \in \tilde{I}(y_{\mathbb{Z}})$. Moreover, from (5.27) and (5.29) we obtain

$$y_{\tilde{\ell}+j} \in V_{j+1}, j = 0, \dots \varkappa - 1, \qquad y_{\tilde{\ell}+j} \in V_0, j = \varkappa, \dots, \varkappa + N_*. \tag{5.30}$$

This shows that the difference of two consecutive indices $\tilde{\ell} < \ell$ in $\tilde{I}(y_{\mathbb{Z}})$ is at least $N = \varkappa + N_*$. Therefore $\tilde{I}(y_{\mathbb{Z}})$ belongs to $\mathbb{Z}(N)$ (cf. (2.9)) and there is a unique sequence $s \in \Omega_N$ such that $\tilde{I}(y_{\mathbb{Z}}) = I(s)$.

The relations (5.30) hold whenever $\ell \in I(s)$. By (5.19) and (5.25) this gives us the estimates

$$\|y_{p+\ell+\nu} - \bar{x}_p\| \le \varepsilon \quad \text{for} \quad \ell \in I(s), p = n_- + 1, \dots, n_+ - 1 \tag{5.31}$$

for the index $\nu = -n_- - 1$ (cf. (2.14)). From this we will derive the estimate

$$T_n := \|y_{n+\nu} - \sum_{m \in I(s)} \bar{x}_{n-m}\| \le C_4 \mathrm{e}^{-\alpha N_4} + C_3|\lambda| + (2C_3 + 1)\varepsilon \quad \text{for} \quad n \in \mathbb{Z}. \tag{5.32}$$

Consider first indices $n = p + \ell$ with $\ell \in I(s)$ and $p = n_- + 1, \dots, n_+ - 1$. Then with (5.24) we find

$$\begin{aligned}
T_n &\le \|y_{p+\ell+\nu} - \bar{x}_p\| + \sum_{m \in I(s), m \neq \ell} \|\bar{x}_{p+\ell-m}\| \\
&\le \varepsilon + C_e \left(\sum_{I(s) \ni m < \ell} \alpha_*^{p+\ell-m} + \sum_{I(s) \ni m > \ell} \alpha_*^{m-\ell-p} \right) \\
&\le \varepsilon + C_e \left(\sum_{\mu \ge 1} \alpha_*^{\mu N + n_- + 1} + \sum_{\mu \ge 1} \alpha_*^{\mu N - n_+ + 1} \right) \\
&= \varepsilon + \frac{C_e}{1 - \alpha_*^N} \left(\alpha_*^{N+n_-+1} + \alpha_*^{N-n_++1} \right) \\
&\le \varepsilon + \frac{2C_e}{1 - \alpha_*} \alpha_*^{N_*}.
\end{aligned} \tag{5.33}$$

Next consider two consecutive indices $\ell < \tilde{\ell}$ in $I(s)$ and $n = p + \ell$ for $p = n_+ - 1, \dots, \tilde{p} = \tilde{\ell} - \ell + n_- + 1$. For these indices we get

$$y_{n+\nu} \in \begin{cases} V_{\varkappa}, & \text{for } p = n_+ - 1, \\ V_1, & \text{for } p = \tilde{p}, \\ V_0, & \text{otherwise,} \end{cases}$$

and we can apply Lemma 14 to this sequence in place of $\tilde{x}_0, \dots, \tilde{x}_K$, where $K = \tilde{\ell} - \ell + 2 - (n_+ - n_-) = \tilde{\ell} - \ell + 1 - \varkappa \geq N_* + 1 = 2N_4 + 1$. With (5.31) this yields the estimate

$$\begin{aligned} &\sup_{j=0,\dots,K} \|y_{\ell+\nu+n_+-1+j} - \bar{x}_{n_++j-1} - \bar{x}_{n_-+j-K+1}\| \\ &\leq C_3 \left(\|y_{\ell+\nu+n_+-1} - \bar{x}_{n_+-1}\| + \|y_{\ell+\nu+n_+-1+K} - \bar{x}_{n_-+1}\| + |\lambda| + \alpha_*^{-K/2} \right) \\ &\leq C_3 \left(2\varepsilon + |\lambda| + \alpha_*^{N_4} \right). \end{aligned} \tag{5.34}$$

Finally, we use this to estimate for $n = p + \ell$ and $p = n_+ - 1, \dots, \tilde{p}$

$$T_n \leq \|y_{n+\nu} - \bar{x}_{n-\ell} - \bar{x}_{n-\tilde{\ell}}\| + \sum_{m \in I(s), m \neq \ell, \tilde{\ell}} \|\bar{x}_{n-m}\|.$$

The first term is handled by (5.34). Further note that

$$\sum_{\tilde{\ell} < m \in I(s)} \|\bar{x}_{n-m}\| \ \leq C_e \sum_{j \geq 1} \alpha_*^{jN_*} \leq \frac{C_e \alpha_*^{N_*}}{1 - \alpha_*} \tag{5.35}$$

and that the same estimate holds for $\ell > m \in I(s)$. Collecting estimates (5.33) to (5.35) we arrive at (5.32):

$$T_n \leq (2C_3 + 1)\varepsilon + C_3|\lambda| + C_3\alpha_*^{N_4} + \frac{2C_e}{1 - \alpha_*}\alpha_*^{2N_4} \leq C_4 \mathrm{e}^{-\alpha N_4} + C_3|\lambda| + (2C_3 + 1)\varepsilon.$$

Finally, we note that (5.32) also holds in case $\tilde{\ell}$ is the smallest index in $I(s)$ or ℓ is the largest index in $I(s)$, respectively. Then one repeats the previous arguments with the formal setting $\ell = -\infty$ resp. $\tilde{\ell} = \infty$ and uses the corresponding one-sided version of Lemma 14.

Step 3: (Construction and estimate of τ and $x_{\mathbb{Z}}$)

We want to find $x_{\mathbb{Z}} \in \ell^\infty(\mathbb{R}^k), \tau \in \ell^\infty(s)$ such that (5.2) holds with $g = 0$. The second term of the operator G in (5.1) vanishes provided we solve

$$\sum_{m \in I(s)} \langle \beta^{-\ell} u_{\mathbb{Z}}, \beta^{-m} u_{\mathbb{Z}} \rangle \tau_m = \langle \beta^{-\ell} u_{\mathbb{Z}}, \beta^{\nu} y_{\mathbb{Z}} - p_{\mathbb{Z}}(s) \rangle, \quad \ell \in I(s), \tag{5.36}$$

and set

$$x_{\mathbb{Z}} = \beta^{\nu} y_{\mathbb{Z}} - p_{\mathbb{Z}}(s) - v_{\mathbb{Z}}(s, \tau). \tag{5.37}$$

By Lemma 12 the linear system (5.36) has a unique solution $\tau \in \ell^\infty(s)$ which satisfies by (5.32), (2.6), (5.15)

$$\begin{aligned}\|\tau\|_\infty &\le 2\|u_{\mathbb{Z}}\|_{\ell^1} \sup_{n\in\mathbb{Z}} \|y_{n+\nu} - \sum_{m\in I(s)} \bar{x}_{n-m}\| \\ &\le 2C_e \frac{1+\alpha_*}{1-\alpha_*} \left(C_4 \mathrm{e}^{-\alpha N_4} + C_3|\lambda| + (2C_3+1)\varepsilon\right).\end{aligned}$$

Using (5.21), (5.22), (5.23) and $C_e\frac{1+\alpha_*}{1-\alpha_*} \le C_5$ we end up with $\|\tau\|_\infty \le \rho_\tau$. Next we estimate $x_{\mathbb{Z}}$ from (5.37). Using (2.6) it is easy to show that

$$\| \sum_{\ell\in I(s)} \beta^{-\ell} u_{\mathbb{Z}}\|_\infty \le C_e \frac{3-\alpha_*}{1-\alpha_*} = C_5. \tag{5.38}$$

Therefore, when using (5.32) again, we find

$$\begin{aligned}\|x_{\mathbb{Z}}\|_\infty &\le \|\beta^\nu y_{\mathbb{Z}} - p_{\mathbb{Z}}(s)\|_\infty + C_5\rho_\tau \\ &\le C_4 \mathrm{e}^{-\alpha N_4} + C_3|\lambda| + (2C_3+1)\varepsilon + C_5\rho_\tau.\end{aligned}$$

The estimates from (5.16), (5.21), (5.22), (5.23) then guarantee $\|x_{\mathbb{Z}}\|_\infty \le \rho_x$.

Therefore, we know that $G_s(x_{\mathbb{Z}}, 0, \tau, \lambda) = 0$ and the tuple $(x_{\mathbb{Z}}, 0, \tau, \lambda)$ lies in the balls in which (5.2) has a unique solution. By uniqueness we conclude $g_s(\tau,\lambda) = 0$ and $x_{\mathbb{Z}} = x_{\mathbb{Z},s}(\tau,\lambda)$ for $\lambda \in \Lambda$. Moreover, by the defining equations (5.36) and (5.37) we obtain that equality (2.14) holds.

Step 4: (Proof of Theorem 1 (ii))
The radius r_τ will be taken such that

$$18C_3(C_0C_2r_\tau^2 + C_5r_\tau) \le \varepsilon. \tag{5.39}$$

Let $\tau \in B_{r_\tau} \subset \ell^\infty(s)$, $\lambda \in \Lambda$ satisfy $g_s(\tau,\lambda) = 0$ for some $s \in \Omega_N$ and let $x_{\mathbb{Z},s}$ be given as in Theorem 11. Then clearly, the sequence

$$y_{\mathbb{Z}} = x_{\mathbb{Z},s}(\tau,\lambda) + p_{\mathbb{Z}}(s) + v_{\mathbb{Z}}(s,\tau)$$

is an orbit of (1.1). It remains to show that $y_n \in U$ for all $n \in \mathbb{Z}$. Application of (5.3) in Theorem 11 and of Lemma 13 yields the estimate

$$\begin{aligned}\|x_{\mathbb{Z},s}(\tau,\lambda)\|_\infty &\le C_0\|G_s(x_{\mathbb{Z},s}(\tau,\lambda), g_s(\tau,\lambda), \tau, \lambda) - G_s(0,0,\tau,\lambda)\|_\infty \\ &= C_0\|F(p_{\mathbb{Z}}(s) + v_{\mathbb{Z}}(s,\tau), \lambda)\|_\infty \\ &\le C_0C_2(|\lambda| + \|\tau\|_\infty^2 + \mathrm{e}^{-\alpha N/2}).\end{aligned} \tag{5.40}$$

From (5.38) we find

$$\|v_{\mathbb{Z}}(s,\tau)\|_\infty \le C_5 r_\tau. \tag{5.41}$$

We estimate the distance of $y_{\mathbb{Z}}$ to the centers of the balls B_j in U by showing for $\nu = -n_- - 1$

$$\|y_{p+\ell+\nu} - \bar{x}_p\| \le \frac{\varepsilon}{6C_3} \quad \text{for} \quad p = n_- + 1, \dots, n_+ - 1, \ell \in I(s). \tag{5.42}$$

Note that the right-hand side is less equal ε since we chose $C_3 \ge 1$ in Lemma 14. Using (5.40), (5.41) and (5.33) we obtain for $\ell \in I(s)$

$$\begin{aligned} \|y_{p+\ell+\nu} - \bar{x}_p\| &= \|x_{p+\ell,s}(\tau,\lambda) + \sum_{m\in I(s), m\neq\ell} \bar{x}_{p+\ell-m} + v_{p+\ell}(s,\tau)\| \\ &\le C_0C_2(|\lambda| + \|\tau\|_\infty^2 + \mathrm{e}^{-\alpha N/2}) + C_5 r_\tau + \frac{2C_e}{1-\alpha_*}\alpha_*^{N_4} \\ &\le C_0C_2|\lambda| + (C_0C_2 r_\tau + C_5) r_\tau + C_6\alpha_*^{N_4}. \end{aligned} \tag{5.43}$$

Conditions (5.22), (5.23) and (5.39) guarantee that (5.42) is satisfied.

Next we consider two consecutive indices $\ell < \tilde{\ell}$ in $I(s)$ and $n = p + \ell$ for $p = n_+ - 1, \dots, \tilde{p} = \tilde{\ell} - \ell + n_- + 1$. In the first step we show that $y_{p+\ell+\nu} \in U_3$. Using $p \ge n_+ - 1$ and $p + \ell - \tilde{\ell} \le n_- + 1$ and (5.35) we estimate similar to (5.43)

$$\begin{aligned} \|y_{p+\ell+\nu}\| &\le \|x_{p+\ell,s}(\tau,\lambda)\| + \|\bar{x}_p\| + \|\bar{x}_{p+\ell-\tilde{\ell}}\| + \sum_{\ell,\tilde{\ell}\neq m\in I(s)} \|\bar{x}_{p+\ell-m}\| + \|v_{p+\ell}(s,\tau)\| \\ &\le C_0C_2(|\lambda| + \|\tau\|_\infty^2 + \mathrm{e}^{-\alpha N/2}) + C_5 r_\tau + \frac{2C_e}{1-\alpha_*}\alpha_*^{N_4} + 2\varepsilon_0 \\ &\le C_0C_2|\lambda| + (C_0C_2 r_\tau + C_5) r_\tau + C_6\alpha_*^{N_4} + 2\varepsilon_0 \\ &\le \frac{\varepsilon}{6C_3} + 2\varepsilon_0 \le 3\varepsilon_0. \end{aligned}$$

Since $B_{3\varepsilon_0} \subset U_3$ this proves our assertion. Now we can invoke Lemma 14 and find as in (5.34)

$$\sup_{j=0,\dots,K} \|y_{\ell+\nu+n_+-1+j} - \bar{x}_{n_++j-1} - \bar{x}_{n_-+j-K+1}\| \le C_3\left(\frac{\varepsilon}{3C_3} + |\lambda| + \alpha_*^{N_4}\right). \tag{5.44}$$

For $j = 0, \dots, N_4$ we have $n_- + j - K + 1 \le -N_4 + n_-$ and hence

$$\|\bar{x}_{n_-+j-K+1}\| \le C_e\mathrm{e}^{\alpha(n_-+N_4-K+1)} \le C_e\alpha_*^{N_4},$$

while for $j = N_4 + 1, \dots K$ we have $n_+ + j - 1 \ge n_+ + N_4$ and hence

$$\|\bar{x}_{n_++j-1}\| \le C_e\alpha_*^{n_++N_4} \le C_e\alpha_*^{N_4}.$$

Combining this with (5.44) we find

$$\begin{aligned} \|y_{p+\ell+\nu} - \bar{x}_p\| &\le \frac{\varepsilon}{3} + C_3|\lambda| + (C_3 + C_e)\alpha_*^{N_4}, \quad p = n_+ - 1, \dots, n_+ - 1 + N_4, \\ \|y_{p+\ell+\nu} - \bar{x}_{p-\tilde{\ell}+\ell}\| &\le \frac{\varepsilon}{3} + C_3|\lambda| + (C_3 + C_e)\alpha_*^{N_4}, \quad p = n_+ + N_4, \dots, \tilde{p}. \end{aligned}$$

We have arranged the constants in (5.22) and (5.23) such that the right hand side is bounded by ε.

For the final step we note that we just have shown (cf. (5.18))

$$y_{p+\ell+\nu} \in \begin{cases} V_{\varkappa}, & \text{for } p = n_+ - 1, \\ V_1, & \text{for } p = \tilde{p} = \tilde{\ell} - \ell + n_- + 1, \\ V_0, & \text{for } p = n_+, \dots, \tilde{\ell} - \ell + n_- \end{cases}$$

for two consecutive indices $\ell < \tilde{\ell}$ in $I(s)$. On the other hand we know from (5.42) that $y_{p+\ell+\nu} \in B_\varepsilon(\bar{x}_p), p = n_- + 1, \dots, n_+ - 1$. Since $y_{\mathbb{Z}}$ is an $f(\cdot, \lambda)$ orbit we conclude by induction from the definition (5.25)

$$y_{p+\ell+\nu} \in V_{p-n_-}, \quad \text{for} \quad p = n_+ - 1, \dots, n_- + 1.$$

Therefore the sequence $y_{\mathbb{Z}}$ lies in U which proves our assertion.

Step 5: (Proof of Theorem 5 (i)) The proof of (2.20),(2.21) is easily accomplished by noting the equivariance relations

$$\begin{aligned} I(\beta s) = I(s) - 1, \quad p_{\mathbb{Z}}(\beta s) = \beta p_{\mathbb{Z}}(s), \quad v_{\mathbb{Z}}(\beta s, \beta\tau) = \beta v_{\mathbb{Z}}(s, \tau), \\ w(\beta s, \beta g) = \beta w(s, g), \quad F(\beta x_{\mathbb{Z}}, \lambda) = \beta F(x_{\mathbb{Z}}, \lambda), \quad \text{and} \\ \langle \beta^\ell u_{\mathbb{Z}}, x_{\mathbb{Z}} \rangle = \langle \beta^{\ell+1} u_{\mathbb{Z}}, \beta x_{\mathbb{Z}} \rangle \quad \text{for} \quad \ell \in I(\beta s) = I(s) - 1. \end{aligned}$$

The assertion then follows by uniqueness from Theorem 11 since neighborhoods are shift invariant as well.

The proof of Theorem 5(ii) will be deferred to the next section.

6 Proof of Reduction Theorem

6.1 Nonlinear estimates

According to (5.1) the Frechet derivative of G_s w.r.t. $x_{\mathbb{Z}}, g$ is given by

$$\begin{aligned} D_{(x,g)} G_s(x_{\mathbb{Z}}, g, \tau, \lambda)(y_{\mathbb{Z}}, h) = \begin{pmatrix} D_x F(p_{\mathbb{Z}}(s) + x_{\mathbb{Z}} + v_{\mathbb{Z}}(s, \tau), \lambda) y_{\mathbb{Z}} + w(s, h) \\ \langle \beta^{-\ell} u_{\mathbb{Z}}, y_{\mathbb{Z}} \rangle, \ \ell \in I(s) \end{pmatrix}, \\ D_x F(x_{\mathbb{Z}}, \lambda) y_{\mathbb{Z}} = (y_{n+1} - f_x(x_n, \lambda) y_n)_{n \in \mathbb{Z}}. \end{aligned} \tag{6.1}$$

The key step in the proof of Theorem 11 will be a uniform bound for the inverse of $D_{(x,g)} G_s(0, 0, 0, 0)$.

Lemma 15 *There exist constants $\hat{C}, \hat{N} > 0$ such that for all $N \geq \hat{N}$, $s \in \Omega_N$ the operator $D_{(x,g)} G_s(0, 0, 0, 0)$ is invertible and satisfies*

$$\|y_{\mathbb{Z}}\|_\infty + \|h\|_\infty \leq \hat{C} \|D_{(x,g)} G_s(0, 0, 0, 0)(y_{\mathbb{Z}}, h)\|, \quad y_{\mathbb{Z}} \in \ell^\infty(\mathbb{R}^k), h \in \ell^\infty(s).$$

Before proving Lemma 15 we finish the proof of Theorem 11.
Proof: Let L_x and L_λ be Lipschitz constants of the Jacobian $f_x(x,\lambda)$ with respect to x and λ in a compact ball that contains the homoclinic orbit in its interior. Then formula (6.1) and the bound (5.38) directly lead to the Lipschitz estimate

$$\begin{aligned} &\|D_{(x,g)}G_s(x^1_{\mathbb{Z}}, g_1, \tau_1, \lambda_1) - D_{(x,g)}G_s(x^2_{\mathbb{Z}}, g_2, \tau_2, \lambda_2)\| \\ &\leq L_x(\|x^1_{\mathbb{Z}} - x^2_{\mathbb{Z}}\|_\infty + C_5\|\tau_1 - \tau_2\|_\infty) + L_\lambda|\lambda_1 - \lambda_2| \end{aligned} \tag{6.2}$$

for all $x^1_{\mathbb{Z}}, x^2_{\mathbb{Z}} \in B_{\rho_x}$, $g_1, g_2 \in \ell^\infty$, $\tau_1, \tau_2 \in B_{\rho_\tau}$, and $\lambda_1, \lambda_2 \in \Lambda_0$ with ρ_x, ρ_τ taken sufficiently small. From Lemma 15 and Lemma 19 we obtain that the operators $D_{(x,g)}G_s(0,0,\tau,\lambda)$ are invertible for $\tau \in B_{\rho_\tau}, \lambda \in B_{\rho_\lambda}$ provided we choose

$$N \geq \hat{N} \quad \text{and} \quad L_x C_5 \rho_\tau + L_\lambda \rho_\lambda \leq \frac{1}{2\hat{C}}.$$

Then we have

$$\|D_{(x,g)}G_s(0,0,\tau,\lambda)^{-1}\| \leq 2\hat{C}, \quad \tau \in B_{\rho_\tau}, \lambda \in B_{\rho_\lambda}.$$

Now we apply Theorem 20 to every operator $F = G_s(\cdot,\cdot,\tau,\lambda)$ in the spaces $Y = Z = \ell^\infty(\mathbb{R}^k) \times \ell^\infty(s)$. Setting $\sigma = \frac{1}{2\hat{C}}$, $y_0 = 0$ and taking $L_x\rho_x \leq \frac{1}{4\hat{C}}$ we find that condition (A.2) is satisfied with $\kappa = \frac{1}{4\hat{C}}$ and $\delta = \rho_x$. Finally, we obtain from Lemma 13 for all $N \geq N_2$,

$$\begin{aligned} \|G_s(0,0,\tau,\lambda)\| &= \|F(p_{\mathbb{Z}}(s) + v_{\mathbb{Z}}(s,\tau),\lambda)\|_\infty \\ &\leq C_2(|\lambda| + \|\tau\|^2_\infty + \mathrm{e}^{-\alpha N/2}) \\ &\leq C_2(\rho_\lambda + \rho_\tau^2 + \mathrm{e}^{-\alpha N/2}). \end{aligned}$$

Now we select $N_0 \geq \max(\hat{N}, N_2)$ and ρ_λ, ρ_τ such that $C_2(\rho_\lambda + \rho_\tau^2 + \mathrm{e}^{-\alpha N_0}) \leq \frac{\rho_x}{4\hat{C}}$. Then we find $\|G_s(0,0,\tau,\lambda)\| \leq (\sigma - \kappa)\delta = \frac{\rho_x}{4\hat{C}}$, for all $N \geq N_0$, i.e. condition (A.3) is satisfied. An application of Theorem 20 finishes the proof. ■

Remark 16 *If instead of Theorem 20 we use a Lipschitz inverse mapping theorem with smooth parameters (cf. [24, Appendix]) then it is easily seen that the solutions $g_s, x_{\mathbb{Z},s}$ are smooth functions of τ and λ.*

Proof: (Theorem 5 (ii))
With c_λ, c_x from (2.18) define $h = h(\tau,\lambda) \in \ell^\infty(s)$ by

$$h_\ell = c_\lambda\lambda + c_x\tau_\ell^2, \quad \ell \in I(s).$$

The idea is to construct elements $y_{\mathbb{Z}} = y_{\mathbb{Z}}(\tau,\lambda) \in \ell^\infty(\mathbb{R}^k)$ and $\gamma = \gamma(\tau,\lambda) \in \ell^\infty(s)$ such that the residual

$$G_s(p_{\mathbb{Z}}(s) + y_{\mathbb{Z}} + v_{\mathbb{Z}}(s,\tau), h + \gamma, \tau, \lambda)$$

and γ are of higher order than $\mathcal{O}(|\lambda| + \|\tau\|_\infty^2)$. Then the assertion follows from (5.3) by comparing them to $x_{\mathbb{Z},s}(\tau,\lambda), g_s(\tau,\lambda)$. We find $y_\mathbb{Z}, \gamma$ by Taylor expansion of F (we abbreviate $F_x^0 = F_x(p_\mathbb{Z}(s), 0)$ etc.)

$$\begin{aligned}
&F(p_\mathbb{Z}(s) + y_\mathbb{Z} + v_\mathbb{Z}(s,\tau), \lambda) = F^0 + F_x^0(y_\mathbb{Z} + v_\mathbb{Z}(s,\tau)) + F_\lambda^0\lambda \\
&+ \frac{1}{2}F_{xx}^0(y_\mathbb{Z} + v_\mathbb{Z}(s,\tau))^2 + F_{x,\lambda}^0(y_\mathbb{Z} + v_\mathbb{Z}(s,\tau))\lambda + \frac{1}{2}F_{\lambda\lambda}^0\lambda^2 \\
&+ \mathcal{O}((|\lambda| + \|\tau\|_\infty + \|y_\mathbb{Z}\|_\infty)^3).
\end{aligned}$$

From the estimates (5.7), (5.8) in the proof of Lemma 13 we have

$$\|F^0\|_\infty = \mathcal{O}(\mathrm{e}^{-\alpha N/2}), \quad \|F_x^0 v_\mathbb{Z}(s,\tau)\| = \mathcal{O}(\mathrm{e}^{-\alpha N/2}\|\tau\|_\infty).$$

In a similar way, using Lipschitz constants for f_λ and f_{xx} we find

$$\begin{aligned}
(F_\lambda^0)_n &= -\sum_{\ell\in I(s)} f_\lambda(\bar{x}_{n-\ell}, 0) + \mathcal{O}(\mathrm{e}^{-\alpha N/2}) \\
(F_{xx}^0(v_\mathbb{Z}(s,\tau))^2)_n &= -\sum_{\ell\in I(s)} \tau_\ell^2 f_{xx}(\bar{x}_{n-\ell}, 0)(u_{n-\ell})^2 + \mathcal{O}(\mathrm{e}^{-\alpha N/2}\|\tau\|_\infty).
\end{aligned}$$

Therefore, Taylor expansion of G_s yields

$$\begin{aligned}
&G_s(p_\mathbb{Z}(s) + y_\mathbb{Z} + v_\mathbb{Z}(s,\tau), h + \gamma, \tau, \lambda) = D_{(x,g)}G_s^0(y_\mathbb{Z}, \gamma) + (\varphi_\mathbb{Z}, 0) \\
&+ \mathcal{O}(\mathrm{e}^{-\alpha N/2} + \|\tau\|_\infty|\lambda| + \|\tau\|_\infty\|y_\mathbb{Z}\|_\infty + \lambda^2 + \|y_\mathbb{Z}\|_\infty^2 + \|\tau\|_\infty^3),
\end{aligned} \tag{6.3}$$

where

$$\varphi_n = \sum_{\ell\in I(s)} \lambda(-f_\lambda(\bar{x}_{n-\ell}, 0) + c_\lambda w_{n-\ell}) + \tau_\ell^2(-\frac{1}{2}f_{xx}(\bar{x}_{n-\ell}, 0)(u_{n-\ell})^2 + c_x w_{n-\ell}).$$

This suggests to define $(y_\mathbb{Z}, \gamma)$ by

$$D_{(x,g)}G_s^0(y_\mathbb{Z}, \gamma) = -(\varphi_\mathbb{Z}, 0). \tag{6.4}$$

From this equation and Lemma 15 we have the estimate

$$\|y_\mathbb{Z}\|_\infty + \|\gamma\|_\infty \le \tilde{C}(|\lambda| + \|\tau\|_\infty^2). \tag{6.5}$$

Taking the inner product of the first coordinate in (6.4) with $\beta^{-\ell}w_\mathbb{Z}, \ell \in I(s)$ and using (2.18), (6.13) leads to the improved estimate

$$\|\gamma\|_\infty \le \tilde{C}\mathrm{e}^{-\alpha N/2}(|\lambda| + \|\tau\|_\infty^2). \tag{6.6}$$

By (6.5), (6.4) the Taylor expansion (6.3) of G_s assumes the form

$$\|G_s(p_\mathbb{Z}(s) + y_\mathbb{Z} + v_\mathbb{Z}(s,\tau), h + \gamma, \tau, \lambda)\| = \mathcal{O}(\mathrm{e}^{-\alpha N/2} + \|\tau\|_\infty|\lambda| + \lambda^2 + \|\tau\|_\infty^3). \tag{6.7}$$

With (5.3) and (6.6) this leads us to the final result

$$\|x_{\mathbb{Z},s}(\tau,\lambda) - y_\mathbb{Z}(\tau,\lambda)\|_\infty + \|g_s(\tau,\lambda) - h(\tau,\lambda)\|_\infty = \mathcal{O}(\mathrm{e}^{-\alpha N/2} + \|\tau\|_\infty|\lambda| + \lambda^2 + \|\tau\|_\infty^3).$$

■

6.2 Linear estimates

In this subsection we prove Lemma 15. For any two integers $n_l \le n_r$ and for any number $a \ge 0$ consider the weight function

$$\omega_n = \omega_n(a, n_l, n_r) = \min\left(\mathrm{e}^{a(n-n_l)}, 1, \mathrm{e}^{a(n_r-n)}\right), \quad n \in \mathbb{Z}. \tag{6.8}$$

Note that $\omega_{\mathbb{Z}}$ has a constant plateau of arbitrary width with exponentially decaying tails on both sides. We also allow $n_l = -\infty$ and $n_r = \infty$ (but neither $n_l = n_r = -\infty$ nor $n_l = n_r = \infty$), in which case $\omega_{\mathbb{Z}}$ has only one-sided decay or degenerates to the maximum norm if $n_l = -\infty$ and $n_r = \infty$. In the following we will suppress the dependence of the norm on the data n_l, n_r, a, but all our estimates will be uniform with respect to

$$-\infty \le n_l \le n_r \le \infty \quad 0 \le a \le a_0 < \alpha, \tag{6.9}$$

where $0 < a_0 < \alpha$ is fixed. The following lemma shows that exponentially decaying kernels preserve the weight.

Lemma 17 *There exists a constant K_0, depending only on a_0, α, such that*

$$\sum_{m\in\mathbb{Z}} \mathrm{e}^{-\alpha|n-m-1|}\omega_m \le K_0\,\omega_n, \quad \textit{for all} \quad n \in \mathbb{Z}$$

and for all weight functions satisfying (6.9).

Proof: We consider

$$\delta_n = \sum_{m\in\mathbb{Z}} \omega_n^{-1}\mathrm{e}^{-\alpha|n-m-1|}\omega_m$$

only for $n \le n_l$ and leave cases $n_l + 1 \le n \le n_r$ and $n_r + 1 \le n$ to the reader.

$$\begin{aligned}
\delta_n =& \sum_{m\le n-1} \mathrm{e}^{a(n_l-n)-\alpha(n-1-m)+a(m-n_l)} + \sum_{m=n}^{n_l-1} \mathrm{e}^{a(n_l-n)-\alpha(m+1-n)+a(m-n_l)} \\
&+ \sum_{m=n_l}^{n_r-1} \mathrm{e}^{a(n_l-n)-\alpha(m+1-n)} + \sum_{m\ge n_r} \mathrm{e}^{a(n_l-n)-\alpha(m+1-n)+a(n_r-m)} \\
=& \mathrm{e}^{-a} \sum_{m\le n-1} \mathrm{e}^{-(\alpha+a)(n-1-m)} + \mathrm{e}^{-\alpha} \sum_{m=n}^{n_l-1} \mathrm{e}^{-(\alpha-a)(m-n)} \\
&+ \mathrm{e}^{-(\alpha-a)(n_l-n)-\alpha} \sum_{m=n_l}^{n_r-1} \mathrm{e}^{-\alpha(m-n_l)} + \mathrm{e}^{-(\alpha-a)(n_l-n)+\alpha(n_l-n_r-1)} \sum_{m\ge n_r} \mathrm{e}^{-(\alpha+a)(m-n_r)} \\
\le& \frac{\mathrm{e}^{-a}+\mathrm{e}^{-\alpha}}{1-\mathrm{e}^{-(\alpha+a)}} + \mathrm{e}^{-\alpha}\left(\frac{1}{1-\mathrm{e}^{-(\alpha-a)}} + \frac{1}{1-\mathrm{e}^{-\alpha}}\right).
\end{aligned}$$

A suitable constant for all cases is $K_0 = 2\frac{1+\mathrm{e}^{-\alpha}}{1-\mathrm{e}^{-\alpha}} + \mathrm{e}^{a_0} + \frac{\mathrm{e}^{a_0}}{1-\mathrm{e}^{-(\alpha-a_0)}}$. ■

With the weights from above we consider the Banach space

$$\ell^\infty_\omega = \{y_\mathbb{Z} \in (\mathbb{R}^k)^\mathbb{Z} : \|y_\mathbb{Z}\|_\omega = \sup_{n\in\mathbb{Z}} \|y_n \omega_n^{-1}\| < \infty\}.$$

Taking the exponent α from (2.6), (2.17) we have the following result for the variational equation (2.5).

Lemma 18 *Let conditions* **A1 - A3** *and* **B4** *hold. Then the linear system*

$$\begin{aligned} y_{n+1} - f_x(\bar{x}_n, 0)y_n + hw_n = r_n, \quad n \in \mathbb{Z} \\ \langle u_\mathbb{Z}, y_\mathbb{Z}\rangle = \gamma \end{aligned} \tag{6.10}$$

has a unique solution $(y_\mathbb{Z}, h) \in \ell^\infty_\omega \times \mathbb{R}$ *for every* $(r_\mathbb{Z}, \gamma) \in \ell^\infty_\omega \times \mathbb{R}$. *Moreover there is a constant* C^* *such that for all weights* (6.8) *with* (6.9),

$$\|y_\mathbb{Z}\|_\omega + |h| \le C^*(\|r_\mathbb{Z}\|_\omega + |\gamma|\|u_\mathbb{Z}\|_\omega). \tag{6.11}$$

If $n_l \le 0 \le n_r$, *then* (6.11) *simplifies to*

$$\|y_\mathbb{Z}\|_\omega + |h| \le C^* \left(\|r_\mathbb{Z}\|_\omega + |\gamma|\right).$$

Proof: Let us abbreviate $A_n = f_x(\bar{x}_n, 0)$, $\mathcal{L}y_\mathbb{Z} = (y_{n+1} - A_n y_n)_{n\in\mathbb{Z}}$ and denote by Φ the solution operator (A.7) of (A.6). From [37, Section 2] (see also [26]) we obtain the following facts. Equation (A.6) has an exponential dichotomy for $n \ge 0$ with data $(K, \alpha, P_n^{+s}, P_n^{+u})$ and for $n \le 0$ with data $(K, \alpha, P_n^{-s}, P_n^{-u})$ (see Definition 21). Due to **B4** we have $\mathcal{R}(P_0^{+s}) \cap \mathcal{R}(P_0^{-u}) = \text{span}\{u_0\} =: Y_0$ and there exist decompositions

$$\mathcal{R}(P_0^{+s}) = Y_0 \oplus Y_+, \quad \mathcal{R}(P_0^{-u}) = Y_0 \oplus Y_-, \quad Y_+ \cap Y_- = \{0\}, \tag{6.12}$$

where

$$\begin{aligned} &k_s = \text{rank}(P_n^{+s}) = \dim(Y_+) + 1, \quad (n \ge 0), \\ &k_u = \text{rank}(P_n^{-u}) = \dim(Y_-) + 1, \quad (n \le 0), \\ &k_u = k - k_s, \quad P_n^{+s} + P_n^{+u} = I \,(n \ge 0),\ P_n^{-s} + P_n^{-u} = I \,(n \le 0). \end{aligned}$$

The operator $\mathcal{L} : \ell^\infty(\mathbb{R}^k) \to \ell^\infty(\mathbb{R}^k)$ is Fredholm of index 0 with

$$\mathcal{N}(\mathcal{L}) = \text{span}\{u_\mathbb{Z}\}, \quad \mathcal{R}(\mathcal{L}) = \{r_\mathbb{Z} \in \ell^\infty(\mathbb{R}^k) : \langle w_\mathbb{Z}, r_\mathbb{Z}\rangle = 0\}. \tag{6.13}$$

One can also choose the ranges of P_0^{+u} and P_0^{-s} such that, in addition to (6.12),

$$\mathbb{R}^k = Y_0 \oplus Y_+ \oplus Y_- \oplus Y_1, \quad \mathcal{R}(P_0^{+u}) = Y_- \oplus Y_1, \quad \mathcal{R}(P_0^{-s}) = Y_+ \oplus Y_1. \tag{6.14}$$

Here $\dim Y_1 = 1$ and one can take $Y_1 = \text{span}\{w_{-1}\}$. Following [37, Lemma 2.7] the general bounded solution of $y_{n+1} - A_n y_n = r_n, n \ge 0$ is given by

$$y_n^+ = \Phi(n, 0)\eta_+ + \sum_{m\ge 0} G_+(n, m+1)r_m, \quad n \ge 0, \quad \eta_+ \in \mathcal{R}(P_0^{+s}) \tag{6.15}$$

with the Green's function defined as follows

$$G_+(n,m) = \begin{cases} \Phi(n,m)P_m^{+s}, & 0 \le m \le n, \\ -\Phi(n,m)P_m^{+u}, & 0 \le n < m. \end{cases} \tag{6.16}$$

Similarly, all bounded solutions of $y_{n+1} - A_n y_n = r_n, n \le -1$ are given by

$$y_n^- = \Phi(n,0)\eta_- + \sum_{m\le -1} G_-(n,m+1)r_m, \quad n \le 0, \quad \eta_- \in \mathcal{R}(P_0^{-u}), \tag{6.17}$$

where

$$G_-(n,m) = \begin{cases} \Phi(n,m)P_m^{-s}, & m \le n \le 0, \\ -\Phi(n,m)P_m^{-u}, & n < m \le 0. \end{cases} \tag{6.18}$$

By the exponential dichotomies the Green's functions satisfy

$$\|G_\pm(n,m)\| \le K\mathrm{e}^{-\alpha|n-m|}, \quad n,m \in \mathbb{Z}_\pm. \tag{6.19}$$

With $u_{\mathbb{Z}}^T y_{\mathbb{Z}} := \langle u_{\mathbb{Z}}, y_{\mathbb{Z}}\rangle$ we may write (6.10) in block operator form as

$$\begin{pmatrix} \mathcal{L} & w_{\mathbb{Z}} \\ u_{\mathbb{Z}}^T & 0 \end{pmatrix} \begin{pmatrix} y_{\mathbb{Z}} \\ h \end{pmatrix} = \begin{pmatrix} r_{\mathbb{Z}} \\ \gamma \end{pmatrix}. \tag{6.20}$$

By the bordering lemma [2, Appendix] the block operator is Fredholm of the same index 0 as $\mathcal{L}$ and, using (6.13), it is a linear homeomorphism in $\ell^\infty(\mathbb{R}^k)\times\mathbb{R}$. Since ℓ^∞_ω is a closed subspace of $\ell^\infty(\mathbb{R}^k)$ it suffices to prove that the unique solution $(y_{\mathbb{Z}}, h)$ of (6.20) in $\ell^\infty(\mathbb{R}^k)\times\mathbb{R}$ satisfies the estimate (6.11) in case $r_{\mathbb{Z}} \in \ell^\infty_\omega$.

Take the inner product of the first equation of (6.10) with $w_{\mathbb{Z}}$. Then (6.13) and the normalization $\|w_{\mathbb{Z}}\|_{\ell^2} = 1$ show $h = \langle w_{\mathbb{Z}}, r_{\mathbb{Z}}\rangle$. Therefore, by (2.17),

$$|h| \le C_e\|r_{\mathbb{Z}}\|_\omega \sum_{n\in\mathbb{Z}} \mathrm{e}^{-\alpha|n|}\omega_n \le C_e\frac{1+\mathrm{e}^{-\alpha}}{1-\mathrm{e}^{-\alpha}}\|r_{\mathbb{Z}}\|_\omega. \tag{6.21}$$

With this h we have $z_{\mathbb{Z}} := r_{\mathbb{Z}} - hw_{\mathbb{Z}} \in \mathcal{R}(\mathcal{L})$ by (6.13). Below we will construct a special solution $\hat{y}_{\mathbb{Z}} \in \ell^\infty(\mathbb{R}^k)$ of $\mathcal{L}\hat{y}_{\mathbb{Z}} = z_{\mathbb{Z}}$ such that for some constant $C > 0$

$$\|\hat{y}_{\mathbb{Z}}\|_\omega \le C\|z_{\mathbb{Z}}\|_\omega. \tag{6.22}$$

By (6.13) and (2.7) the solution of (6.20) is given by

$$(y_{\mathbb{Z}}, h) = (\hat{y}_{\mathbb{Z}} + cu_{\mathbb{Z}}, h), \quad c = \gamma - \langle u_{\mathbb{Z}}, \hat{y}_{\mathbb{Z}}\rangle, \quad h = \langle w_{\mathbb{Z}}, r_{\mathbb{Z}}\rangle. \tag{6.23}$$

From the exponential decay (2.6), (2.17) and Lemma 17, applied to the kernel $\mathrm{e}^{-\alpha(|n|+|m|)} \le \mathrm{e}^{\alpha}\mathrm{e}^{-\alpha|n-m-1|}$, we obtain with $C' = C_e\mathrm{e}^\alpha K_0$,

$$\|\langle u_{\mathbb{Z}}, \hat{y}_{\mathbb{Z}}\rangle u_{\mathbb{Z}}\|_\omega \le C'\|\hat{y}_{\mathbb{Z}}\|_\omega, \quad \|\langle w_{\mathbb{Z}}, r_{\mathbb{Z}}\rangle w_{\mathbb{Z}}\|_\omega \le C'\|r_{\mathbb{Z}}\|_\omega.$$

Then (6.21)-(6.23) yield the assertion

$$\|y_{\mathbb{Z}}\|_\omega \le (1+C')\|\hat{y}_{\mathbb{Z}}\|_\omega + |\gamma|\|u_{\mathbb{Z}}\|_\omega \le C(1+C')^2\|r_{\mathbb{Z}}\|_\omega + |\gamma|\|u_{\mathbb{Z}}\|_\omega.$$

It remains to construct $\hat{y}_{\mathbb{Z}}$ with $\mathcal{L}\hat{y}_{\mathbb{Z}} = z_{\mathbb{Z}}$ and (6.22). We determine $\eta_+ \in \mathcal{R}(P_0^{+s})$ and $\eta_- \in \mathcal{R}(P_0^{-u})$ such that $\hat{y}_n = y_n^+, n \ge 0$ with y_n^+ from (6.15), and $\hat{y}_n = y_n^-, n \le 0$ with y_n^- from (6.17), and such that the definitions coincide at $n = 0$. The last condition holds if and only if

$$\eta_+ - \eta_- = \sum_{m\le -1} G_-(0,m+1)z_m - \sum_{m\ge 0} G_+(0,m+1)z_m =: \Delta_0. \tag{6.24}$$

By (6.16), (6.18), (6.14) the first sum on the right is in $Y_+ \oplus Y_1$ and the second sum is in $Y_- \oplus Y_1$ while the left-hand side is in $Y_0 \oplus Y_- \oplus Y_+$. Since $z_{\mathbb{Z}} \in \mathcal{R}(\mathcal{L})$ holds, equation (6.24) has a solution and thus $\Delta_0 \in Y_+ \oplus Y_-$. We conclude from (6.14) that $\eta_+ = P_0^{+s}\Delta_0$ and $\eta_- = -P_0^{-u}\Delta_0$ are the unique solutions of (6.24). With (6.19) and Lemma 17 we estimate for $n \ge 0$

$$\|\hat{y}_n\|\omega_n^{-1} \le K\|z_{\mathbb{Z}}\|_\omega \sum_{m\ge 0} \omega_n^{-1}\mathrm{e}^{-\alpha|n-m-1|}\omega_m \le KK_0\|z_{\mathbb{Z}}\|_\omega.$$

An analogous estimate holds for $n \le 0$ and this completes the proof. ■

Proof: (Lemma 15) We use Lemma 19 and construct an approximate right inverse B_+ of $D_{(x,g)}G_s^0 = D_{(x,g)}G_s(0,0,0,0)$. For any $\ell \in I(s)$ we define the interval $J(\ell) = \{\ell_-, \dots, \ell, \dots, \ell_+\}$ where right and left neighbors are given by

$$\ell_+ = \begin{cases} \infty, & \text{if} \quad \ell = \max I(s), \\ \ell + N_*, & \text{otherwise,} \end{cases} \tag{6.25}$$

$$\ell_- = \begin{cases} -\infty, & \text{if} \quad \ell = \min I(s), \\ \max\{\tilde{\ell}_+ : \tilde{\ell} \in I(s), \tilde{\ell} < \ell\} + 1, & \text{otherwise.} \end{cases} \tag{6.26}$$

Note that the sets $J(\ell), \ell \in I(s)$ define a partitioning of $\mathbb{Z}$. In the following we consider $N \ge \hat{N} = 2N_* + 1$ which implies $\ell - \ell_- \ge \ell_+ - \ell \ge N_*$. During the proof N_* will be taken sufficiently large. Given an element $(r_{\mathbb{Z}}, \gamma) \in \ell^\infty(\mathbb{R}^k) \times \ell^\infty(s)$, we decompose

$$r_{\mathbb{Z}} = \sum_{\ell \in I(s)} \mathbb{1}_{J(\ell)} r_{\mathbb{Z}}, \quad \text{where} \quad (\mathbb{1}_{J(\ell)})_n = \begin{cases} 1, & n \in J(\ell), \\ 0, & \text{else} \end{cases}$$

is the characteristic function of $J(\ell)$. Let B_0 denote the solution operator of (6.20), then we set

$$(y_{\mathbb{Z}}^\ell, h_\ell) = B_0(\beta^\ell \mathbb{1}_{J(\ell)} r_{\mathbb{Z}}, \gamma_\ell) \quad \text{for} \quad \ell \in I(s), \tag{6.27}$$

and define B_+ as a blockwise inverse via

$$B_+(r_{\mathbb{Z}},\gamma)=(y_{\mathbb{Z}},h)=(\sum_{\ell\in I(s)}\beta^{-\ell}y^{\ell}_{\mathbb{Z}},(h_\ell)_{\ell\in I(s)}). \tag{6.28}$$

Using Lemma 18 with the settings $n_l=\ell_--\ell$, $n_r=\ell_+-\ell$ we obtain a bound

$$\|y^{\ell}_{\mathbb{Z}}\|_\omega+|h_\ell|\le C^*\left(\|\beta^{\ell}\mathbb{1}_{J(\ell)}r_{\mathbb{Z}}\|_\omega+|\gamma_\ell|\right)\le C^*\left(\|r_{\mathbb{Z}}\|_\infty+|\gamma_\ell|\right). \tag{6.29}$$

Let us abbreviate the weights from (6.8),

$$\omega_{n,\ell}=\omega_n(a,\ell_-,\ell_+),\quad n\in\mathbb{Z},\ell\in I(s).$$

Then equation (6.28) and (6.29) lead to the estimate

$$\|y_n\|\le\|\sum_{\ell\in I(s)}y^{\ell}_{n-\ell}\|\le C^*\left(\|r_{\mathbb{Z}}\|_\infty+\|\gamma\|_\infty\right)\sum_{\ell\in I(s)}\omega_{n,\ell},$$

For $2\mathrm{e}^{-aN^*}\le 1$ the last sum is bounded by $1+4\mathrm{e}^{-a}$ and (6.29) yields

$$\|B_+(r_{\mathbb{Z}},\gamma)\|=\|y_{\mathbb{Z}}\|_\infty+\|h\|_\infty\le(2C^*+1+4\mathrm{e}^{-a})(\|r_{\mathbb{Z}}\|_\infty+\|\gamma\|_\infty). \tag{6.30}$$

In the next step we show for N^* sufficiently large,

$$\|(r_{\mathbb{Z}},\gamma)-D_{(x,g)}G^0_sB_+(r_{\mathbb{Z}},\gamma)\|\le\frac{1}{2}(\|r_{\mathbb{Z}}\|_\infty+\|\gamma\|_\infty), \tag{6.31}$$

which by (A.1), (6.30) gives the desired estimate

$$\|(D_{(x,g)}G^0_s)^{-1}\|\le 2(2C^*+1+4\mathrm{e}^{-a}).$$

We introduce $(\tilde r_{\mathbb{Z}},\tilde\gamma)=(r_{\mathbb{Z}},\gamma)-D_{(x,g)}G^0_s(y_{\mathbb{Z}},h)$. From (6.28) and the variational equation in (6.27) we have

$$\begin{aligned}\tilde r_n=&r_n-\Big(\sum_{m\in I(s)}y^m_{n+1-m}-f_x(\sum_{p\in I(s)}\bar x_{n-p},0)y_n+\sum_{m\in I(s)}h_mw_{n-m}\Big)\\=&\sum_{m\in I(s)}\Big[f_x(\sum_{p\in I(s)}\bar x_{n-p},0)-f_x(\bar x_{n-m},0)\Big]y^m_{n-m}.\end{aligned}$$

For $n\in\mathbb{Z}$ there exists a unique $\ell\in I(s)$ such that $n\in J(\ell)$. Define the neighborhood $\mathcal{U}(\ell)$ of ℓ by $\mathcal{U}(\ell)=\{\hat\ell,\ell,\tilde\ell\}$ with left neighbor $\hat\ell=\sup\{m\in I(s):m<\ell\}$ and right neighbor $\tilde\ell=\inf\{m\in I(s):m>\ell\}$ (as usual let $\hat\ell=-\infty$ and $\tilde\ell=\infty$ if the sets are empty). Using the Lipschitz constant L_x of f_x and (2.12), (6.29) we obtain

$$\begin{aligned}\|\tilde r_n\|\le&L_x\Big(\sum_{m\in I(s)\setminus\mathcal{U}(\ell)}\|y^m_{n-m}\|\sum_{m\neq p\in I(s)}\|\bar x_{n-p}\|+\sum_{m\in\mathcal{U}(\ell)}\|y^m_{n-m}\|\sum_{m\neq p\in I(s)}\|\bar x_{n-p}\|\Big)\\\le&L_xC^*(\|r_{\mathbb{Z}}\|_\infty+\|\gamma\|_\infty)\Big\{\bar C\sum_{m\in I(s)\setminus\mathcal{U}(\ell)}\omega_{n,m}+\sum_{\ell\neq p\in I(s)}\|\bar x_{n-p}\|\\&+\omega_{n,\tilde\ell}\Big(\|\bar x_{n-\ell}\|+\sum_{p\in I(s)\setminus\{\ell,\tilde\ell\}}\|\bar x_{n-p}\|\Big)+\omega_{n,\hat\ell}\Big(\|\bar x_{n-\ell}\|+\sum_{p\in I(s)\setminus\{\ell,\hat\ell\}}\|\bar x_{n-p}\|\Big)\Big\}.\end{aligned}$$

We show that the terms in $\{\dots\}$ are of order $\mathcal{O}(\mathrm{e}^{-aN_*})$ so that the contraction estimate (6.31) holds for the first component if N^* is sufficiently large. A critical term on the right-hand side is

$$\omega_{n,\tilde{\ell}}\|\bar{x}_{n-\ell}\| \le C_e\mathrm{e}^{-\alpha|n-\ell|+a(n-\tilde{\ell}_-)} \le C_e\mathrm{e}^{a(\ell-\tilde{\ell}_-)} \le C_e\mathrm{e}^{-aN^*}, \quad \ell_- \le n \le \ell_+. \tag{6.32}$$

The term $\omega_{n,\hat{\ell}}\|\bar{x}_{n-\ell}\|$ is handled analogously. Further,

$$\begin{aligned}\sum_{\ell\neq p\in I(s)} \|\bar{x}_{n-p}\| &\le C_e\Big(\sum_{\ell>p\in I(s)} \mathrm{e}^{-\alpha(n-p)} + \sum_{\ell<p\in I(s)} \mathrm{e}^{-\alpha(p-n)}\Big)\\ &\le C_e\Big(\sum_{\ell>p\in I(s)} \mathrm{e}^{-\alpha(\ell_--p)} + \sum_{\ell<p\in I(s)} \mathrm{e}^{-\alpha(p-\ell_+)}\Big) \le 2C_e\frac{\mathrm{e}^{-\alpha N_*}}{1-\mathrm{e}^{-\alpha}}.\end{aligned}$$

The remaining terms allow similar estimates since n always lies in an exponential decaying tail of the weights and of the shifted homoclinic orbits. Finally, we use (2.6) and (6.27), (6.29) for $\ell \in I(s)$,

$$\begin{aligned}|\gamma_\ell - \langle\beta^{-\ell}u_{\mathbb{Z}}, y_{\mathbb{Z}}\rangle| &= |\sum_{n\in\mathbb{Z}}\langle u_{n-\ell}, \sum_{\ell\neq m\in I(s)} y^m_{n-m}\rangle|\\ &\le C_eC^*(\|r_{\mathbb{Z}}\|_\infty + \|\gamma\|_\infty)\sum_{n\in\mathbb{Z}}\mathrm{e}^{-\alpha|n-\ell|}\sum_{\ell\neq m\in I(s)}\omega_{n,m}.\end{aligned}$$

We estimate the remaining sum by using (6.32)

$$\begin{aligned}\sum_{n\in\mathbb{Z}}\mathrm{e}^{-\alpha|n-\ell|}\sum_{\ell\neq m\in I(s)}\omega_{n,m} &\le \sum_{n=\ell_-}^{\ell_+}\mathrm{e}^{-\alpha|n-\ell|}\Big(\omega_{n,\tilde{\ell}} + \omega_{n,\hat{\ell}} + \sum_{m\in I(s)\setminus\mathcal{U}(\ell)}\omega_{n,m}\Big)\\ &\quad + C\Big(\sum_{n=\ell_+}^{\infty}\mathrm{e}^{-\alpha(n-\ell)} + \sum_{n=-\infty}^{\ell_--1}\mathrm{e}^{-\alpha(\ell-n)}\Big).\end{aligned}$$

The last two terms are $\mathcal{O}(\mathrm{e}^{-\alpha N^*})$ since $\ell_+-\ell \ge N^*$ and $\ell-\ell_- \ge N^*$. Furthermore, we have for $\ell_- \le n \le \ell_+$

$$\begin{aligned}\sum_{m\in I(s)\setminus\mathcal{U}(\ell)}\omega_{n,m} &\le \sum_{\tilde{\ell}<m\in I(s)}\mathrm{e}^{a(n-m_-)} + \sum_{\hat{\ell}>m\in I(s)}\mathrm{e}^{a(m_+-n)}\\ &\le \sum_{\tilde{\ell}<m\in I(s)}\mathrm{e}^{a(\ell_--m_-)} + \sum_{\hat{\ell}>m\in I(s)}\mathrm{e}^{a(m_+-\ell_+)} \le \frac{2\mathrm{e}^{-2aN^*}}{1-\mathrm{e}^{-aN^*}}.\end{aligned}$$

Our final estimate is

$$\begin{aligned}\sum_{n=\ell_-}^{\ell_+}\mathrm{e}^{-\alpha|n-\ell|}\omega_{n,\tilde{\ell}} &\le \sum_{n=\ell_-}^{\ell}\mathrm{e}^{-\alpha(\ell-n)+a(n-\tilde{\ell}_-)} + \sum_{n=\ell+1}^{\ell_+}\mathrm{e}^{-\alpha(n-\ell)+a(n-\tilde{\ell}_-)}\\ &\le \frac{\mathrm{e}^{-aN^*}}{1-\mathrm{e}^{-\alpha}} + \frac{\mathrm{e}^{-aN^*}}{1-\mathrm{e}^{-(\alpha-a)}}.\end{aligned}$$

The term $\sum_{n=\ell_-}^{\ell_+} \mathrm{e}^{-\alpha|n-\ell|}\omega_{n,\hat{\ell}}$ is estimated in a similar way. This finishes the proof of (6.31).

We take the same $B_- = B_+$ as an approximate left inverse in Lemma 19. It is convenient to require $0 < 2a \le a_0 < \alpha$ instead of (6.9). Given $(y_{\mathbb{Z}}, h) \in \ell^\infty(\mathbb{R}^k) \times \ell^\infty(s)$, we set

$$(\eta_{\mathbb{Z}}, t) = B_+ D_{(x,g)} G_s^0(y_{\mathbb{Z}}, h),$$

then it is sufficient to show

$$\|\eta_{\mathbb{Z}} - y_{\mathbb{Z}}\|_\infty + \|t - h\|_\infty \le \mathcal{O}(\mathrm{e}^{-(\alpha-a)N_*})(\|y_{\mathbb{Z}}\|_\infty + \|h\|_\infty). \tag{6.33}$$

For a fixed $\ell \in I(s)$ we consider first the case

$$y_n = 0 \quad (n \le \ell_- \text{ and } n > \ell_+), \quad h_m = 0 \quad (m \ne \ell), \tag{6.34}$$

and prove the stronger estimate (recall $\hat{N} = 2N_* + 1$)

$$\|\eta_{\mathbb{Z}} - y_{\mathbb{Z}}\|_\omega + |t_\ell - h_\ell| + \sup_{\ell \ne m \in I(s)} |t_m| \mathrm{e}^{\alpha(|m-\ell|-\hat{N})} \le \mathcal{O}(\mathrm{e}^{-\alpha N_*})(\|y_{\mathbb{Z}}\|_\omega + |h_\ell|), \tag{6.35}$$

where $\omega_n = \omega_n(a, \ell_-, \ell_+)$, see (6.8). Then we consider the case

$$y_n = 0 \quad (n \ne \ell_-), \quad h = 0 \tag{6.36}$$

and prove the estimate

$$\|\eta_{\mathbb{Z}} - y_{\mathbb{Z}}\|_\omega + \sup_{m \in \mathbb{Z}} |t_m| \mathrm{e}^{a|m-\ell_-|} \le \mathcal{O}(\mathrm{e}^{-aN_*}) \|y_{\mathbb{Z}}\|_\omega, \tag{6.37}$$

where $\omega_n = \omega(a, \ell_-, \ell_-)$. Let us first show that the general case (6.33) follows from (6.35) and (6.37). With $J^0(\ell) = \{\ell_- + 1, \dots, \ell_+\}$, $J^1(\ell) = \{\ell_-\}$ we decompose

$$(y_{\mathbb{Z}}, h) = \sum_{m \in I(s)} \left[(\mathbb{1}_{J^0(m)} y_{\mathbb{Z}}, h_m \mathbb{1}_{\{m\}}) + (\mathbb{1}_{J^1(m)} y_{\mathbb{Z}}, 0) \right]$$

and define

$$(\eta_{\mathbb{Z}}, t) = \sum_{m \in I(s)} B_+ D_{(x,g)} G_s^0 \left[(\mathbb{1}_{J^0(m)} y_{\mathbb{Z}}, h_m \mathbb{1}_{\{m\}}) + (\mathbb{1}_{J^1(m)} y_{\mathbb{Z}}, 0) \right].$$

Similar to the proof of (6.31) we combine the local estimates (6.35) and (6.37),

$$\begin{aligned}
\|y_n - \eta_n\| &= \mathcal{O}(\mathrm{e}^{-aN_*}) \sum_{m \in I(s)} \big[\omega_n(a, m_-, m_+)(\|\mathbb{1}_{J^0(m)} y_{\mathbb{Z}}\|_\omega + |h_m|) \\
&\qquad + \omega_n(a, m_-, m_-) \|\mathbb{1}_{\{m_-\}} y_{\mathbb{Z}}\|_\omega \big] \\
&= \mathcal{O}(\mathrm{e}^{-aN_*})(\|y_{\mathbb{Z}}\|_\infty + \|h\|_\infty) \sum_{m \in I(s)} \left[\omega_n(a, m_-, m_+) + \omega_n(a, m_-, m_-) \right]. \\
&= \mathcal{O}(\mathrm{e}^{-aN_*})(\|y_{\mathbb{Z}}\|_\infty + \|h\|_\infty).
\end{aligned}$$

Using the exponential weights of t_m in (6.35) and (6.37) leads to the same estimate for $\|h-t\|_\infty$ and (6.33) is proved.

For the proof of (6.35) let $\gamma_m = \langle \beta^{-m} u_{\mathbb{Z}}, y_{\mathbb{Z}} \rangle$ and note that (6.34) implies $r_n = 0$ for $n \notin J(\ell)$. Hence $\eta^\ell_{\mathbb{Z}} = \beta^\ell y_{\mathbb{Z}}$ satisfies

$$\eta^\ell_{n+1} - f_x(\bar{x}_n, 0)\eta^\ell_n + h_\ell w_n = r_{n+\ell} + [f_x(p_{n+\ell}(s), 0) - f_x(\bar{x}_n, 0)]\,\eta^\ell_n.$$

Using Lemma 18 and a Lipschitz estimate for f_x we can compare with the solution $(y^\ell_{\mathbb{Z}}, t_\ell) = B_0(\beta^\ell \mathbb{1}_{J(\ell)} r_{\mathbb{Z}}, \gamma_\ell)$ of (6.27). This leads to

$$\|\beta^{-\ell} y^\ell_{\mathbb{Z}} - y_{\mathbb{Z}}\|_\omega + |t_\ell - h_\ell| = \mathcal{O}(\mathrm{e}^{-\alpha N^*})(\|y_{\mathbb{Z}}\|_\omega + |h_\ell|).$$

For the solutions $(y^m_{\mathbb{Z}}, t_m) = B_0(\beta^m \mathbb{1}_{J(m)} r_{\mathbb{Z}}, \gamma_m) = B_0(0, \gamma_m)$ with $m \neq \ell$ Lemma 18 gives

$$\|\beta^{-m} y^m_{\mathbb{Z}}\|_\omega + |t_m| \leq C^* |\gamma_m| \leq C_e \|y_{\mathbb{Z}}\|_\omega \sum_{n=\ell_-+1}^{\ell_+} \mathrm{e}^{-\alpha|n-m|} = \mathcal{O}(\mathrm{e}^{-\alpha(|m-\ell|-N^*)})\|y_{\mathbb{Z}}\|_\omega.$$

Collecting the last two estimates we find that $(\eta_{\mathbb{Z}}, t) = (\sum_{m\in I(s)} \beta^{-m} y^m_{\mathbb{Z}}, (t_m)_{m\in I(s)})$ (cf. (6.28)) satisfies inequality (6.35).

In case condition (6.36) holds, let

$$r_n = (D_x F(p_{\mathbb{Z}}(s), 0) y_{\mathbb{Z}})_n \ (n \in \mathbb{Z}), \quad \gamma_m = \langle \beta^{-m} u_{\mathbb{Z}}, y_{\mathbb{Z}} \rangle \ (m \in I(s)),$$

and note $r_n = 0$ for $n \neq \ell_-, \ell_- - 1$ as well as

$$r_{\ell_-} = -f_x(p_{\ell_-}(s), 0) y_{\ell_-}, \quad r_{\ell_- - 1} = y_{\ell_-}. \tag{6.38}$$

Moreover,

$$|\gamma_m| = |u^T_{\ell_- - m} y_{\ell_-}| \leq C_e \mathrm{e}^{-\alpha|\ell_- - m|} \|y_{\ell_-}\|, \quad m \in I(s). \tag{6.39}$$

As in (6.27) let $(y^m_{\mathbb{Z}}, t_m) = B_0(\beta^m \mathbb{1}_{J(m)} r_{\mathbb{Z}}, \gamma_m)$ for $m \in I(s)$. Recall $\ell_- - 1 = \hat{\ell}_+$ from (6.26) where $\hat{\ell} \in I(s)$ is the left neighbor of ℓ. For $m \neq \ell, \hat{\ell}$ we have $y^m_{\mathbb{Z}} = \beta^{-m} \gamma_m u_{\mathbb{Z}}$, $t_m = 0$ by (6.23) and therefore by (6.39),

$$\|y^m_{\mathbb{Z}}\|_\omega \leq C_e^2 \|y_{\ell_-}\| \mathrm{e}^{-\alpha|\ell_- - m|} \sup_{n\in\mathbb{Z}} \mathrm{e}^{-\alpha|n-m|+a|n-\ell_-|} = \mathcal{O}(\mathrm{e}^{-(\alpha-a)|\ell_- - m|})\|y_{\ell_-}\|. \tag{6.40}$$

We introduce the weights $\omega^*_n = \omega_n(2a, \ell_- - \ell, \ell_- - \ell)$. For $m = \ell$ we use (6.39) and Lemma 18 with ω^*,

$$\begin{aligned} \|y^\ell_{\mathbb{Z}}\|_{\omega^*} \leq & C^* \left(\|\beta^\ell \mathbb{1}_{J(\ell)} r_{\mathbb{Z}}\|_{\omega^*} + |\gamma_\ell| \|u_{\mathbb{Z}}\|_{\omega^*} \right) \\ \leq & C^* \left(1 + C \mathrm{e}^{-(\alpha-2a)|\ell_- - \ell|} \right) \|y_{\ell_-}\| \leq C \|y_{\ell_-}\|. \end{aligned} \tag{6.41}$$

In a similar manner,

$$\|y^{\hat{\ell}}_{\mathbb{Z}}\|_{\hat{\omega}^*} \leq C \|y_{\ell_-}\| \tag{6.42}$$

holds for the weights $\hat{\omega}_n^* = \omega_n(2a, \hat{\ell}_+ - \hat{\ell}, \hat{\ell}_+ - \hat{\ell})$. The t-values satisfy

$$\begin{aligned} |t_\ell| &= |u_{\ell_- - \ell}^T f_x(p_{\ell_-}(s), 0) y_{\ell_-}| \le C\mathrm{e}^{-\alpha|\ell_- - \ell|}\|y_{\ell_-}\|, \\ |t_{\hat{\ell}}| &= |u_{\hat{\ell} - \hat{\ell}_+}^T y_{\ell_-}| \le C\mathrm{e}^{-\alpha|\hat{\ell} - \hat{\ell}_+|}\|y_{\ell_-}\|. \end{aligned} \tag{6.43}$$

In particular, this proves the t-estimates in (6.37). Next we estimate the difference $d_{\mathbb{Z}} = \beta^{-\ell} y_{\mathbb{Z}}^{\ell} + \beta^{-\hat{\ell}} y_{\mathbb{Z}}^{\hat{\ell}} - y_{\mathbb{Z}}$ by using the exponential dichotomy on $\mathbb{Z}$ for the constant coefficient operator $\mathcal{L}_0 y_{\mathbb{Z}} = (y_{n+1} - A y_n)_{n\in\mathbb{Z}}$, $A = f_x(0,0)$. From (6.38) and the definition of $y_{\mathbb{Z}}^{\ell}, y_{\mathbb{Z}}^{\hat{\ell}}$ we find

$$\begin{aligned} d_{n+1} - A d_n = {} & (f_x(\bar{x}_{n-\ell}, 0) - A) y_{n-\ell}^{\ell} + (f_x(\bar{x}_{n-\hat{\ell}}, 0) - A) y_{n-\hat{\ell}}^{\hat{\ell}} \\ & - t_\ell w_{n-\ell} - t_{\hat{\ell}} w_{n-\hat{\ell}} + (A - f_x(p_{\ell_-}(s), 0)) \delta_{n,\ell_-} y_{\ell_-} = \sum_{i=1}^{5} T_i. \end{aligned}$$

For every term we show $\|T_i\| = \mathcal{O}(\mathrm{e}^{-aN_*})\omega_n \|y_{\ell_-}\|$ with weights $\omega_n = \mathrm{e}^{-a|n-\ell_-|}$. In fact, our previous estimates (6.41) - (6.43) yield

$$\begin{aligned} \|T_1\|\omega_n^{-1} &\le C\|\bar{x}_{n-\ell}\|\mathrm{e}^{-a|n-\ell_-|}\|y_{\mathbb{Z}}^{\ell}\|_{\omega^*} \\ &\le C\|y_{\ell_-}\|\mathrm{e}^{-\alpha|n-\ell|-a|n-\ell_-|} \le C\mathrm{e}^{-a|\ell-\ell_-|}\|y_{\ell_-}\| = \mathcal{O}(\mathrm{e}^{-aN_*})\|y_{\ell_-}\|, \\ \|T_2\|\omega_n^{-1} &\le C\mathrm{e}^{-\alpha|n-\hat{\ell}|+a|n-\ell_-|-2a|n-\hat{\ell}_+|}\|y_{\ell_-}\| \le C\mathrm{e}^{-a|\hat{\ell}-\hat{\ell}_+|}\|y_{\ell_-}\| = \mathcal{O}(\mathrm{e}^{-aN_*})\|y_{\ell_-}\|, \\ \|T_3\|\omega_n^{-1} &\le C|t_\ell|\mathrm{e}^{a|n-\ell_-|-\alpha|n-\ell|} \le C\mathrm{e}^{-(\alpha-a)|\ell-\ell_-|}\|y_{\ell_-}\| = \mathcal{O}(\mathrm{e}^{-aN_*})\|y_{\ell_-}\|, \\ \|T_4\|\omega_n^{-1} &\le C|t_\ell|\mathrm{e}^{a|n-\ell_-|-\alpha|n-\hat{\ell}|} \le C\mathrm{e}^{-(\alpha-a)|\hat{\ell}-\hat{\ell}_+|}\|y_{\ell_-}\| = \mathcal{O}(\mathrm{e}^{-aN_*})\|y_{\ell_-}\|, \\ \|T_5\|\omega_n^{-1} &\le C\|\sum_{m\in I(s)} \bar{x}_{\ell_- - m}\|\|y_{\ell_-}\| = \mathcal{O}(\mathrm{e}^{-\alpha N_*})\|y_{\ell_-}\|. \end{aligned}$$

Since the operator $\mathcal{L}_0$ has a Green's function with an exponentially decaying kernel we infer from Lemma 17

$$\|d_{\mathbb{Z}}\|_\omega \le C\mathrm{e}^{-aN_*}\|y_{\ell_-}\|.$$

Combining this with (6.40) gives

$$\begin{aligned} \|\sum_{m\in I(s)} y_{n-m}^m - y_n\| &\le \|d_n\| + \sum_{\ell,\hat{\ell}\neq m\in I(s)} \|y_{n-m}^m\| \\ &\le C\Big(\omega_n \mathrm{e}^{-aN_*} + \sum_{\ell,\hat{\ell}\neq m\in I(s)} \mathrm{e}^{-a|\ell_- - m|}\Big)\|y_{\ell_-}\| = \mathcal{O}(\mathrm{e}^{-aN_*})\omega_n\|y_{\ell_-}\|. \end{aligned}$$

This finally proves the y-estimates in (6.37). ■

A Auxiliary results

Lemma 19 *(Banach Lemma) Let X, Y be Banach spaces and let $A \in L[X,Y]$, $B_-, B_+ \in L[Y,X]$ be bounded linear operators such that*

$$\|I_Y - AB_+\| < 1, \quad \|I_X - B_-A\| < 1.$$

Then A is a homeomorphism with

$$\|A^{-1}\| \leq \min\left(\frac{\|B_+\|}{1-\|I_Y - AB_+\|}, \frac{\|B_-\|}{1-\|I_X - B_-A\|}\right). \tag{A.1}$$

Proof: Note that $y = (I_Y - AB_+)y + r$ has a unique solution y for every $r \in Y$. Then y satisfies

$$\|y\| \leq \frac{\|r\|}{1-\|I_Y - AB_+\|}$$

and $x = B_+y$ solves $Ax = r$. To prove uniqueness, note that any solution x of $Ax = r$ solves $x = (I_X - B_-A)x + B_-r$. Since $I_X - B_-A$ is also contractive the solution is unique and the estimates follow. ■

A key tool in the proofs of Lemma 14 and Theorem 11 is the following quantitative version of the Lipschitz inverse mapping theorem, cf. [24].

Theorem 20 *Assume Y and Z are Banach spaces, $F \in C^1(Y,Z)$ and $F'(y_0)$ is for $y_0 \in Y$ a homeomorphism. Let $\kappa,\ \sigma,\ \delta > 0$ be three constants, such that the following estimates hold:*

$$\left\|F'(y) - F'(y_0)\right\| \leq \kappa < \sigma \leq \frac{1}{\left\|F'(y_0)^{-1}\right\|} \quad \forall y \in B_\delta(y_0), \tag{A.2}$$

$$\left\|F(y_0)\right\| \leq (\sigma - \kappa)\delta. \tag{A.3}$$

Then F has a unique zero $\bar{y} \in B_\delta(y_0)$ and the following inequalities are satisfied

$$\left\|F'(y)^{-1}\right\| \leq \frac{1}{\sigma - \kappa} \quad \forall y \in B_\delta(y_0), \tag{A.4}$$

$$\|y_1 - y_2\| \leq \frac{1}{\sigma - \kappa}\left\|F(y_1) - F(y_2)\right\| \quad \forall y_1,\ y_2 \in B_\delta(y_0). \tag{A.5}$$

We collect some well known results on exponential dichotomies from [37]. Denote by Φ the solution operator of the linear difference equation

$$y_{n+1} = A_n y_n, \quad n \in \mathbb{Z}, \tag{A.6}$$

which is defined as

$$\Phi(n,m) := \begin{cases} A_{n-1}\dots A_m, & \text{for } n > m, \\ I, & \text{for } n = m, \\ A_n^{-1}\dots A_{m-1}^{-1}, & \text{for } n < m. \end{cases} \tag{A.7}$$

Definition 21 *The linear difference equation* (A.6) *with invertible matrices* $A_n \in \mathbb{R}^{k,k}$ *has an* ***exponential dichotomy*** *with data* $(K, \alpha, P_n^s, P_n^u)$ *on an interval* $J \subset \mathbb{Z}$*, if there exist two families of projectors* P_n^s *and* $P_n^u = I - P_n^s$ *and constants* $K,\ \alpha > 0$*, such that the following statements hold:*

$$P_n^s \Phi(n,m) = \Phi(n,m) P_m^s \quad \forall n, m \in J,$$

$$\begin{aligned} \|\Phi(n,m)P_m^s\| &\leq K\mathrm{e}^{-\alpha(n-m)} \\ \|\Phi(m,n)P_n^u\| &\leq K\mathrm{e}^{-\alpha(n-m)} \end{aligned} \qquad \forall n \geq m,\ n, m \in J.$$

Theorem 22 *(Roughness Theorem, cf. [37, Proposition 2.10]) Assume that the difference equation*

$$y_{n+1} = A_n y_n, \quad A_n \in \mathbb{R}^{k,k} \text{ invertible}, \quad \|A_n^{-1}\| \leq M \ \forall n \in J$$

with an interval $J \subseteq \mathbb{Z}$*, has an exponential dichotomy with data* $(K, \alpha, P_n^s, P_n^u)$*. Suppose* $B_n \in \mathbb{R}^{k,k}$ *satisfies* $\|B_n\| \leq b$ *for all* $n \in J$ *with a sufficiently small* b*. Then* $A_n + B_n$ *is invertible and the perturbed difference equation*

$$y_{n+1} = (A_n + B_n) y_n$$

has an exponential dichotomy on J*.*

Acknowledgment

The authors thank an anonymous referee for several helpful suggestions.

References

[1] E. L. Allgower and K. Georg. *Numerical Continuation Methods*. Springer-Verlag, Berlin, 1990. An introduction.

[2] W.-J. Beyn. The numerical computation of connecting orbits in dynamical systems. *IMA J. Numer. Anal.*, 10:379–405, 1990.

[3] W.-J. Beyn, T. Hüls, J.-M. Kleinkauf, and Y. Zou. Numerical analysis of degenerate connecting orbits for maps. *Internat. J. Bifur. Chaos Appl. Sci. Engrg.*, 14(10):3385–3407, 2004.

[4] W.-J. Beyn and J.-M. Kleinkauf. The numerical computation of homoclinic orbits for maps. *SIAM J. Numer. Anal.*, 34(3):1207–1236, 1997.

[5] C. Bonatti, L. J. Díaz, and M. Viana. *Dynamics beyond uniform hyperbolicity*, volume 102 of *Encyclopaedia of Mathematical Sciences*. Springer-Verlag, Berlin, 2005. A global geometric and probabilistic perspective, Mathematical Physics, III.

[6] H. Broer, C. Simó, and J. C. Tatjer. Towards global models near homoclinic tangencies of dissipative diffeomorphisms. *Nonlinearity*, 11(3):667–770, 1998.

[7] P. Collins. Symbolic dynamics from homoclinic tangles. *Internat. J. Bifur. Chaos Appl. Sci. Engrg.*, 12(3):605–617, 2002.

[8] P. Collins. Dynamics of surface diffeomorphisms relative to homoclinic and heteroclinic orbits. *Dyn. Syst.*, 19(1):1–39, 2004.

[9] P. Collins and B. Krauskopf. Entropy and bifurcations in a chaotic laser. *Phys. Rev. E (3)*, 66(5):056201, 8, 2002.

[10] D. W. Decker and H. B. Keller. Path following near bifurcation. *Comm. Pure Appl. Math.*, 34(2):149–175, 1981.

[11] R. L. Devaney. *An Introduction to Chaotic Dynamical Systems*. Addison-Wesley Studies in Nonlinearity. Addison-Wesley Publishing Company Advanced Book Program, Redwood City, CA, second edition, 1989.

[12] J. P. England, B. Krauskopf, and H. M. Osinga. Computing one-dimensional stable manifolds and stable sets of planar maps without the inverse. *SIAM J. Appl. Dyn. Syst.*, 3(2):161–190 (electronic), 2004.

[13] R. K. Ghaziani, W. Govaerts, Y. A. Kuznetsov, and H. G. E. Meijer. Numerical continuation of connecting orbits of maps in MATLAB. *J. Difference Equ. Appl.*, 15(8-9):849–875, 2009.

[14] M. Golubitsky and D. G. Schaeffer. *Singularities and groups in bifurcation theory. Vol. I*, volume 51 of *Applied Mathematical Sciences*. Springer-Verlag, New York, 1985.

[15] S. V. Gonchenko, D. V. Turaev, and L. P. Shilnikov. On the dynamic properties of diffeomorphisms with homoclinic tangencies. *Sovrem. Mat. Prilozh.*, 7:91–117, 2003. J. Math. Sci. (N.Y.) 126, 1317-1343 (2005).

[16] V. S. Gonchenko, Y. A. Kuznetsov, and H. G. E. Meijer. Generalized Hénon map and bifurcations of homoclinic tangencies. *SIAM J. Appl. Dyn. Syst.*, 4(2):407–436, 2005.

[17] W. Govaerts. *Numerical methods for bifurcations of dynamical equilibria*. Society for Industrial and Applied Mathematics (SIAM), Philadelphia, PA, 2000.

[18] J. Guckenheimer and P. Holmes. *Nonlinear Oscillations, Dynamical Systems, and Bifurcations of Vector Fields*, volume 42 of *Applied Mathematical Sciences*. Springer-Verlag, New York, 1990.

[19] J. K. Hale and H. Koçak. *Dynamics and Bifurcations*, volume 3 of *Texts in Applied Mathematics*. Springer-Verlag, New York, 1991.

[20] M. Hénon. A two-dimensional mapping with a strange attractor. *Comm. Math. Phys.*, 50(1):69–77, 1976.

[21] A. J. Homburg and B. Krauskopf. Resonant homoclinic flip bifurcations. *J. Dynam. Differential Equations*, 12(4):807–850, 2000.

[22] A. J. Homburg and B. Sandstede. Homoclinic and heteroclinic bifurcations in vector fields. In H. Broer, F. Takens, and B. Hasselblatt, editors, *Handbook of Dynamical Systems III,*, pages 379–524. Elsevier, 2010.

[23] T. Hüls. Homoclinic trajectories of non-autonomous maps. *J. Difference Equ. Appl.*, 17(1):9–31, 2011.

[24] M. C. Irwin. *Smooth dynamical systems*, volume 17 of *Advanced Series in Nonlinear Dynamics*. World Scientific Publishing Co. Inc., River Edge, NJ, 2001. Reprint of the 1980 original, With a foreword by R. S. MacKay.

[25] H. B. Keller. Numerical solution of bifurcation and nonlinear eigenvalue problems. In *Applications of bifurcation theory (Proc. Advanced Sem., Univ. Wisconsin, Madison, Wis., 1976)*, pages 359–384. Publ. Math. Res. Center, No. 38. Academic Press, New York, 1977.

[26] J.-M. Kleinkauf. The numerical computation and geometrical analysis of heteroclinic tangencies. Technical Report 98-048, SFB 343, 1998.

[27] J.-M. Kleinkauf. *Numerische Analyse tangentialer homokliner Orbits*. PhD thesis, Universität Bielefeld, 1998. Shaker Verlag, Aachen.

[28] J. Knobloch. Chaotic behaviour near non-transversal homoclinic points with quadratic tangency. *J. Difference Equ. Appl.*, 12(10):1037–1056, 2006.

[29] J. Knobloch and T. Rieß. Lin's method for heteroclinic chains involving periodic orbits. *Nonlinearity*, 23(1):23–54, 2010.

[30] B. Krauskopf, H. M. Osinga, E. J. Doedel, M. E. Henderson, J. Guckenheimer, A. Vladimirsky, M. Dellnitz, and O. Junge. A survey of methods for computing (un)stable manifolds of vector fields. *Internat. J. Bifur. Chaos Appl. Sci. Engrg.*, 15(3):763–791, 2005.

[31] B. Krauskopf and T. Rieß. A Lin's method approach to finding and continuing heteroclinic connections involving periodic orbits. *Nonlinearity*, 21(8):1655–1690, 2008.

[32] D. Lind and B. Marcus. *An introduction to symbolic dynamics and coding*. Cambridge University Press, Cambridge, 1995.

[33] C. Mira. *Chaotic dynamics*. World Scientific Publishing Co., Singapore, 1987. From the one-dimensional endomorphism to the two-dimensional diffeomorphism.

[34] B. E. Oldeman, A. R. Champneys, and B. Krauskopf. Homoclinic branch switching: a numerical implementation of Lin's method. *Internat. J. Bifur. Chaos Appl. Sci. Engrg.*, 13(10):2977–2999, 2003.

[35] J. Palis and F. Takens. *Hyperbolicity and Sensitive Chaotic Dynamics at Homoclinic Bifurcations*, volume 35 of *Cambridge Studies in Advanced Mathematics*. Cambridge University Press, Cambridge, 1993.

[36] K. Palmer. *Shadowing in dynamical systems*, volume 501 of *Mathematics and its Applications*. Kluwer Academic Publishers, Dordrecht, 2000. Theory and applications.

[37] K. J. Palmer. Exponential dichotomies, the shadowing lemma and transversal homoclinic points. In *Dynamics reported, Vol. 1*, pages 265–306. Teubner, Stuttgart, 1988.

[38] S. Y. Pilyugin. *Shadowing in Dynamical Systems*, volume 1706 of *Lecture Notes in Mathematics*. Springer-Verlag, Berlin, 1999.

[39] R. J. Sacker and G. R. Sell. A spectral theory for linear differential systems. *J. Differential Equations*, 27(3):320–358, 1978.

[40] B. Sandstede. Constructing dynamical systems having homoclinic bifurcation points of codimension two. *J. Dynam. Differential Equations*, 9(2):269–288, 1997.

[41] M. Shub. *Global stability of dynamical systems*. Springer-Verlag, New York, 1987. With the collaboration of Albert Fathi and Rémi Langevin, Translated from the French by Joseph Christy.

[42] L. P. Šil'nikov. Existence of a countable set of periodic motions in a neighborhood of a homoclinic curve. *Dokl. Akad. Nauk SSSR*, 172:298–301, 1967. Soviet Math. Dokl. 8 (1967), 102–106.

[43] S. Smale. Differentiable dynamical systems. *Bull. Amer. Math. Soc.*, 73:747–817, 1967.